Zfp318 controls the recallability of memory B cells

Yifeng Wang[1,2,3,4]*, Wen Shao[1,2,3,4]*, Xin Liu[1,2,3,4], Qingtai Liang[4], Jiaqi Lei[5], Miao Mei[6], Ying Li[7], Xu Tan[1,6], Guocan Yu[4,5], Li Yu[1,7,8], Linqi Zhang[4], and Hai Qi[1,2,3,4,7,8,9]

[1]Tsinghua-Peking Center for Life Sciences, Beijing 100084, China

[2]Changping Laboratory, Yard 28, Science Park Rd., Changping District, Beijing 102206, China

[3]Laboratory of Dynamic Immunobiology, Institute for Immunology, Tsinghua University, Beijing 100084, China

[4]Department of Basic Medical Sciences, School of Medicine, Tsinghua University, Beijing 100084, China

[5]Key Laboratory of Bioorganic Phosphorus Chemistry & Chemical Biology, Department of Chemistry, Tsinghua University, Beijing 100084, China

[6]School of Pharmaceutical Sciences, Tsinghua University, Beijing 100084, China

[7]School of Life Sciences, Tsinghua University, Beijing 100084, China

[8]Beijing Frontier Research Center for Biological Structure, Tsinghua University, Beijing 100084, China

[9]Beijing Key Laboratory for Immunological Research on Chronic Diseases, Tsinghua University, Beijing 100084, China

* These authors contribute equally to this work.

Correspondence should be addressed to Hai Qi (Email: qihai@tsinghua.edu.cn)

Abstract

Memory B cells (MBCs) are important for efficacious antibody-based vaccines and develop via germinal center (GC)-dependent and -independent routes. We find all MBCs are not equally recallable by antigen. Zfp318, a transcription regulator of spermatogenesis and IgD expression, is not expressed in GC B cells but upregulated in MBCs. GC-derived MBCs are far more recallable than GC-independent MBCs in a Zfp318-dependent manner. Zfp318 expression is inhibited by BCR but promoted by CD40 signaling, while its levels are positively correlated with B-cell receptor affinities. Enforced Zfp318 expression markedly increases the recallability of GC-independent MBCs. Zfp318-deficient MBCs show reduced expression of mitochondrion-related genes, exhibit lower mitochondrial membrane potentials, contain more structurally compromised mitochondria, and are susceptible to activation-induced cell death. The abundance of Zfp318-expressing MBCs positively correlates with the quality of vaccine-induced antibody immunity. Therefore, Zfp318 defines the recallability of the MBC compartment and represents a key regulator of humoral immune memory.

Introduction

Memory B cells (MBCs) play a key role in vaccine-induced protection from infectious diseases. In a standard prime-boost regimen, primary immunization leads to the development of MBCs that, upon boost, are re-activated to produce long-lived plasma cells (LLPCs) to sustain serum antibody titers for an extended period of time [1–3]. Some re-activated MBCs participate in secondary germinal center (GC) reaction [4–7], and by undergoing diversification and selection again may lead to emergence of antibodies that recognize pathogen variants and those heavily mutated, broadly neutralizing antibodies against mutating viruses [8,9]. Therefore, successful prime-boost vaccines depend on functional MBCs of appropriate quality developed during the prime. Many efforts are devoted to understanding how reactivated MBCs decide to differentiate into PCs or to develop into secondary GCs. However, it is not yet established that all MBCs are equally responsive to antigen, that is, capable of being reactivated or recallable by antigen to become PCs or GCs.

Antigen-specific MBCs develop from both GC-independent and -dependent routes [5,10–13], with the former affording potentially a broader spectrum of reactivities toward the antigen and the latter a more focused, affinity-matured response. GC-independent MBCs contain mainly unswitched IgM^+ cells together with a minor component of IgG^+ MBCs, whereas GC-dependent MBCs are composed of both switched and IgM^+ MBCs [12,13]. GC-independent MBCs are often the numerically dominant fraction among all antigen-binding MBCs [4,5,12]. It is not understood whether and how GC-independent and -dependent MBCs differentially contribute to the recall response upon booster immunization. Human studies suggest that long-lived and functionally recallable MBCs are primarily those with GC experience [14–16], whereas mouse work suggests that GC-independent MBCs can be recalled in lymphopenic hosts [13].

We and others have previously shown that $CD38^+Fas^+GL7^+$ GC cells contain precursors to MBCs [17–19]. By adoptive transfer into normal mice, we showed that these GC memory precursor (GCMP) cells can reconstitute memory capable of generating both secondary GCs and PCs upon antigen re-exposure [19]. By analyzing these cells in detail, we find that Zfp318, a transcription regulator that is known to control spermatogenesis[20] and IgD expression in naïve B cells[21,22], controls MBC recallability.

Results

In GCMP cells, we noticed upregulation of *Zfp318*, the gene coding for a zinc finger protein that regulates IgD expression in naïve B cells [21,22]. We verified that *Zfp318* expression was very low in bulk GC ($CD19^+IgD^-CD38^-Fas^+GL7^+$) B cells, became upregulated in $CD19^+IgD^-CD38^+Fas^+GL7^+$ GCMP cells, maintained in the bulk of $CD19^+IgD^-CD38^+Fas^-GL7^-$ antigen-binding MBCs, and decreased again in the bulk of $CD138^+B220^-$ plasma cells (PCs; Fig. S1a-b). The only known function of Zfp318 in the immune system is to promote IgD expression by repressing recognition of a transcription termination site [22]. However, GCMP cells or MBCs do not express

IgD. A deficiency in IgD expression causes a minor defect in antibody affinity maturation during the primary response and has almost no impact on the secondary response [23]. This curious contradiction led us to suspect that Zfp318 might play a role in regulating MBC development and/or function.

GC-derived MBCs express Zfp318.

We constructed a loss-of-function *Zfp318* allele that conditionally expresses a fluorescent reporter together with a cell-ablation apparatus (Fig. S1c). Immediately downstream of the transcription start site of the *Zfp318* gene, we inserted a construct containing a STOP cassette flanked by two flox sites, which is followed sequentially by the coding sequence for diphtheria toxin receptor (DTR), the coding sequence for the self-cleaving 2A peptide of *Thosea asigna* virus, and the coding sequence for tdTomato (Fig. S1c). This mutant allele cannot express *Zfp318* gene, but it permits expression of both DTR and tdTomato under the endogenous *Zfp318* locus control after excision of the STOP cassette by a Cre driver. We denote this modified allele ZSDAT and further bred it with AID-Cre transgenic mice to obtain AID-Cre;*Zfp318*$^{ZSDAT/+}$ mice in which GC-derived cells become tdTomato^{+} when their *Zfp318* promoter is transcriptionally active. By quantitative RT-PCR analyses of sort-purified cells, we verified that tdTomato fluorescence faithfully reported *Zfp318* expression and co-segregated with DTR expression (Fig. S1d-e), as designed. Accordingly, DT treatment led to complete deletion of tdTomato^{+} MBCs within 12 h *in vivo* (Fig. S1f).

In these reporter mice, the bulk of Fas^{+}GL7^{+} GCs had only a small fraction of tdTomato^{+} cells, most of which were CD38^{+} memory precursors. MBC, splenic PC (SPPC) and bone-marrow PC (BMPC) compartments all contained a fraction of tdTomato^{+} cells (Fig. 1a-b; gated as in Fig. S1a). The relative abundance of the tdTomato^{+} fraction in these compartments increased at later time points, reaching ~15-20% of NP-binding MBCs, SPPCs or BMPCs 2 months after immunization (Fig. 1b). We further bred AID-Cre;*Zfp318*$^{ZSDAT/+}$ with the Rosa26-Ai3 reporter line so that EYFP fluorescence could be used to approximately indicate a GC origin. As shown in Fig. 1c-d, essentially all Zfp318-expressing tdTomato^{+} MBCs were EYFP^{+} GC-derived, and DT treatment specifically deleted these GC-derived MBCs. Finally, as compared to tdTomato^{-} counterparts, NIP-binding tdTomato^{+} MBCs more frequently harbored the affinity-enhancing W33L mutation on both day 14 and 28 after NP-KLH immunization in AID-Cre;*Zfp318*$^{ZSDAT/+}$ mice (Fig. 1e). From day 14 to 28, the overall Ig somatic mutation load in tdTomato^{+} MBCs markedly increased (from 2.2±0.2 to 4.2±0.5), whereas the mutation load in tdTomato^{-} MBCs showed minimal change (0.7±0.1 to 1.1±0.2; Fig. 1e), indicating that the latter contains predominantly GC-independent MBCs and MBCs formed early in the GC reaction. Therefore, in AID-Cre;*Zfp318*$^{ZSDAT/+}$ reporter mice, tdTomato reports Zfp318 expression and captures most of GC-derived MBCs. Using this system, we went on to probe MBC development and recall function and examine a potential role for Zfp318.

MBC development does not require Zfp318.

It has previously been reported that, in the complete absence of Zfp318, B cells

develop normally [22]. The replacement of one wildtype *Zfp318* allele with the ZSDAT allele did not alter the primary response to NP-KLH immunization, as evidenced by the similar GC, SPPC, BMPC and MBC abundance in AID-Cre;*Zfp318*$^{ZSDAT/+}$ and control AID-Cre mice (Fig. S2). Similar titers and affinities of NP-specific antibodies were found in these mice (Fig. S2c and S2f). AID-Cre;*Zfp318*$^{ZSDAT/ZSDAT}$ mice, which lack Zfp318 entirely, showed no defect in mounting the primary response (Fig. S3). Therefore, Zfp318 is not required for the primary B cell response and not required for MBC development.

Zfp318-expressing GC-derived MBCs are dominant in antigen recall.

Taking advantage of the cell ablation apparatus in the ZSDAT allele, we evaluated the relative contribution of GC-dependent and -independent MBCs to the overall recall response, an issue that has not been addressed in normal animals [1,3,24]. We enriched NIP-binding MBCs from AID-Cre;*Zfp318*$^{ZSDAT/+}$ mice 30 days after NP-KLH immunization, and these MBCs were transferred into CD45.1 mice that were primed with ovalbumin (OVA) 30 days earlier (Fig. 2a). Recipient mice were immunized with NP-OVA and, a day later, treated with either DT to delete GC-derived MBCs or treated with PBS as control. As shown in Fig. 2b-c, whereas donor MBCs in the PBS-treated group abundantly produced secondary GCs and PCs, the DT-treated group barely produced any response. Therefore, within the MBC compartment, Zfp318-expressing GC-derived MBCs are the dominant recall responder in producing both secondary GCs and PCs. This superior recallability of GC-derived MBCs was not peculiar to the NP hapten-specific response, as it was also observed with influenza hemagglutinin as the model antigen (Fig. S4a-c).

Zfp318 is required for MBC recall.

To test whether Zfp318 directly regulates MBC recall functions, we enriched MBCs from AID-Cre;*Zfp318*$^{ZSDAT/ZSDAT}$;Rosa26-Ai3 or control AID-Cre;Rosa26-Ai3 mice that were immunized with NP-KLH 30 days previously. An equal number of NIP-binding MBCs were transferred into CD45.1 recipient mice that had been primed with OVA (Fig. 3a), with each recipient receiving an equal number of NIP-binding MBCs. Seven days after NP-OVA immunization of these recipients, donor-derived GCs and PCs were identified by CD45.2 (Fig. 3b). Consistent with the functional dominance of GC-derived MBCs in recall, EYFP^{+} cells constituted the vast majority among all CD45.2^{+} donor-derived GCs or PCs (Fig. 3c), even though EYFP^{+} GC-derived MBCs only accounted for 10-20% of all antigen-binding MBCs being re-activated (Fig. 1). Importantly, the absence of Zfp318 led to a strikingly diminished recall generation of both secondary GCs and PCs (Fig. 3d), suggesting a fundamental block of the response even before the choice between GC and PC development.

Consistent with previous findings based on a Zfp318-deficient line [21], B cells from *Zfp318*$^{ZSDAT/ZSDAT}$ mice lack IgD expression (not shown). However, the lack of IgD expression in naïve B cells was not the underlying reason for diminished recall by Zfp318-deficient MBCs, because MBCs derived from *Ighd*$^{-/-}$ or wildtype naïve B cells mounted a comparable recall response (Fig. S5).

To rule out potential influence of affinity variations, we additionally conducted adoptive transfer experiments using BCR knock-in transgenic B1-8^{hi} cells. Zfp318-deficient (ubGFP;AID-Cre;*Zfp318*$^{ZSDAT/ZSDAT}$) and Zfp318-heterozygous (ubGFP;AID-Cre;*Zfp318*$^{ZSDAT/+}$) B1-8^{hi} cells were first activated in B6 hosts. A month later, NP-binding, tdTomato^{+} MBCs were sort-purified from these mice and transferred into a second group of B6 recipients that were primed with OVA (Fig. S6a). Those tdTomato^{+} Zfp318-deficient MBCs were Zfp318-want-to-express cells that cannot express Zfp318. Seven days after NP-OVA immunization of this second group of B6 recipients, we found that secondary GCs and PCs generated by Zfp318-deficient MBCs were markedly diminished as well (Fig. S6b-c). Taken together, these data demonstrate Zfp318 is required for functional memory recall.

Zfp318 confers increased recallability to GC-independent MBCs

To test whether Zfp318 is sufficient for enhancing the recallability of GC-independent MBCs, which are otherwise functionally inferior, we created a transgenic system that allows inducible expression of Zfp318 in a cell type-specific manner. As shown in Fig. 4a, a single copy of the Tet-on expression cassette was knocked-in to the *Col1a1* safe locus; the resultant strain, termed *Col1a1*$^{Teton\text{-}zfp318}$, was bred with *Rosa26*$^{LSL\text{-}rtTA3}$ mice. This combined genetic apparatus was then introduced into *CD79a*$^{Cre/+}$ B1-8^{hi} mice. We used *Col1a1*$^{Teto\text{-}zfp318/+}$;*Rosa26*$^{LSL\text{-}rtTA3/+}$;*CD79a*$^{Cre/+}$ or control *Rosa26*$^{LSL\text{-}rtTA3/+}$;*CD79a*$^{Cre/+}$ B1-8^{hi} mice as donors of MBCs in adoptive transfer experiments (Fig. 4b).

To enrich GC-derived MBCs without the ZSDAT reporter, we resorted to the CD73 marker, which has previously been associated with GC-dependent MBCs [12,25]. In AID-Cre;*Zfp318*$^{ZSDAT/+}$ mice, a ~75% majority of Zfp318-expressing MBCs were CD73^{+}, while ~65% of CD73^{+} MBCs were Zfp318-expressing (Fig. S7a-b). Therefore, CD73^{+} MBCs in immunized mice could approximate a 70%-pure population of GC-derived MBCs, while the CD73^{-} population contains ~90% GC-independent MBCs. Sort-purified CD73^{+} MBCs expressed higher levels of Zfp318 (Fig. 4c-d). Importantly, in recall assays by adoptive transfer (Fig. S7c), CD73^{+} MBCs markedly outperformed their CD73^{-} counterpart in producing secondary GCs and PCs (Fig. S7d-e).

In order to obtain sufficient numbers of sorted CD73^{+} or CD73^{-} B1-8^{hi} MBCs required for testing recall in lymphoreplete hosts, we harvested MBCs on day 7 post primary immunization. The recall function of tdTomato^{+} MBCs isolated at this earlier time point depended on Zfp318 (Fig. S6d-g), just as MBCs isolated on day 30.

After these validations, we sort-purified CD73^{-} B1-8^{hi} MBCs of the *Col1a1*$^{Teto\text{-}zfp318/+}$;*Rosa26*$^{LSL\text{-}rtTA3/+}$;*CD79a*$^{Cre/+}$ genotype, control CD73^{-} B1-8^{hi} MBCs of a *Rosa26*$^{LSL\text{-}rtTA3/+}$;*CD79a*$^{Cre/+}$ genotype, and control CD73^{+} MBCs of a *Rosa26*$^{LSL\text{-}rtTA3/+}$;*CD79a*$^{Cre/+}$ genotype. These three groups of cells were transferred into three groups of CD45.1 mice, which were all primed with OVA and treated with doxycycline (Fig. 4b). At the time of cell transfer, recipient mice were challenged with NP-OVA. As shown in Fig. 4e-f, while CD73^{-} MBCs were functionally inferior to CD73^{+} MBCs in recall, as expected, induced Zfp318 expression conferred a much improved

recallability to CD73$^-$ MBCs in generating secondary GCs and PCs. Combined together, these genetic evidences demonstrate that Zfp318 is not only necessary but also sufficient for the MBC recallability.

Zfp318 expression is promoted by T-cell help.

A major difference between GC-independent and GC-dependent MBCs is the cumulative amount of T cell help they experience. Within GCs, Zfp318 is upregulated in GCMP cells (Fig. S1). To explore the possibility that T cell help drives Zfp318 upregulation, sort-purified light-zone or dark-zone GC B cells were treated with either anti-Ig to mimic antigen stimulation of BCR or agonistic anti-CD40 to mimic T-cell help via CD40 ligand. Naïve B cells were tested in parallel. Whereas Zfp318 was downregulated by BCR stimulation in all types of B cells tested (Fig. 5a), it was upregulated by CD40 signaling and only in LZ GC B cells (Fig. 5b). Furthermore, we observed a strong positive correlation between the level of Zfp318 expression (tdTomato fluorescence) and the relative affinity of individual tdTomato$^+$ GC-derived MBCs, as reflected by normalizing the NIP antigen-binding intensity against the level of surface Ig expression (Fig. 5c). This correlation was not peculiar to the NP hapten-specific response but also observed in hemagglutinin-binding tdTomato$^+$ GC-derived MBCs following PR8 influenza infection (Fig. 5d). Together, these data suggest that T-cell help upregulates Zfp318 expression and promotes the recallability of GC-dependent MBCs.

Zfp318 safeguards mitochondrial integrity and attenuates activation-induced cell death.

Given the fact that Zfp318-deficient MBCs mounts almost no recall response, Zfp318 likely controls a very upstream event in the recall, possibly executing a binary decision between life and death for MBCs upon re-stimulation. To explore this issue, we sought to define transcriptomic features that distinguish Zfp318-sufficient from Zfp318-deficient MBCs by mRNA sequencing. We set up 3 systems to compare MBCs that differ in levels of Zfp318 expression and show distinct recallabilities (Fig. 6a-c). First, sort-purified EYFP$^+$ NIP-binding MBCs from AID-Cre;*Zfp318*$^{ZSDAT/ZSDAT}$;Rosa26-Ai3 mice (Zfp318-deficient) were compared to those from control AID-Cre;Rosa26-Ai3 mice (Zfp318-sufficient) 30 days after NP-KLH immunization (Fig. 6a; corresponding MBC recall experiment in Fig. 3). Second, sort-purified tdTomato$^+$ B1-8^{hi} MBCs of AID-Cre;*Zfp318*$^{ZSDAT/+}$ mice (Zfp318-heterozygous) were compared to those of AID-Cre;*Zfp318*$^{ZSDAT/ZSDAT}$ mice (Zfp318-deficient) 7 days after immunization (Fig. 6b; corresponding MBC recall experiment in Fig. S7d-g). Third, sort-purified tdTomato$^+$ B1-8^{hi} MBCs of AID-Cre;*Col1a1*$^{Teto-zfp318/+}$;*Rosa26*$^{LSL-rtTA3/+}$;*Zfp318*$^{ZSDAT/ZSDAT}$ mice (Zfp318-induced) or control AID-Cre;*Col1a1*$^{+/+}$;*Rosa26*$^{LSL-rtTA3/+}$;*Zfp318*$^{ZSDAT/ZSDAT}$ mice (Zfp318-deficient) 7 days after immunization under doxycycline treatment (Fig. 6c). The effect of exogenous Zfp318 in conferring recallability was verified in Fig. 4.

By K-means clustering analyses, we observed a total of 12 gene clusters that were differentially expressed in these three datasets (Fig. S8a). The cluster A of 812 genes

showed consistent downregulation, and the cluster B of 343 genes showed consistent upregulation in Zfp318-deficient MBCs as compared to Zfp318-sufficient, Zfp318-heterozygous or Zfp318-induced MBCs (Fig. 6d). By gene ontology analysis, the cluster A was highly enriched with mitochondrion-related, nuclear genome-encoded genes, including those that support mitochondrial ATP synthesis-coupled proton transport and mitochondrial translation and those mediating cellular responses to DNA damage and oxidative stress (Fig. 6e). The cluster B was enriched with genes involved in cytoplasmic translation (Fig. S8b). Gene set enrichment analysis further showed, in Zfp318-deficient MBCs, downregulation of 16 mitochondrion-related gene sets that impinge on all aspects of mitochondrial structure and function (Fig. 6f). In particular, Zfp318-deficient MBCs exhibited markedly reduced expression of genes orchestrating mitochondrial translation (Fig. S8c), ATP synthesis (Fig. S8d), defense against oxidative stress (Fig. S8e-f) and negative regulation of cytochrome c release (Fig. 6f and S8g).

Consistent with these transcriptomic features, mitochondria of Zfp318-deficient MBCs are structurally and functionally compromised. By MitoSpy staining, Zfp318-deficient MBCs consistently exhibited lower mitochondrial membrane potentials (Fig. 6g). By electron microscopy, Zfp318-deficient MBCs contained fewer mitochondria (Fig. 6h-i), and a significantly larger fraction of mitochondria showing a swollen morphology with few intact cristae (Fig. 6j-k), structural deformation that often results from abnormally increased mitochondrial permeabilities. On the other hand, Zfp318-deficient naïve B cells do not show any numerical reduction or structural compromise (Fig. S8h; Fig. 6i), indicating an MBC-specific function of Zfp318 in safeguards mitochondrial integrity.

Because BCR activation significantly increases mitochondrial activities and inherently causes mitochondrial stress, which can lead to B cell death without timely rescue by T cell help [26], we tested whether Zfp318-deficient MBCs may become more sensitive to activation-induced cell death. Consistent with this possibility, brief activation with an anti-Ig antibody led to significantly increased Caspase 3 activation in Zfp318-deficient MBCs (Fig. 6l). Conversely, induction of exogenous Zfp318 in Zfp318-deficient MBCs reduced apoptosis caused by BCR stimulation (Fig. 6m). Together, these data support that Zfp318 promotes mitochondrial integrity and counteracts activation-induced cell death in MBCs.

Re-programming of GC-independent MBCs by Zfp318

While GC-independent MBCs are less recallable, they may harbor clones that react to antigenic variants of pathogens [27], a feature that could be exploited for development of broadly neutralizing vaccines. To establish a proof-of-principle method for re-programing the recallability of GC-independent MBCs, we resorted to mRNA transfection by lipid nanoparticles (LNP). Polyclonal MBCs resulting from primary immunization were transfected with LNPs containing Zfp318- or GFP-coding mRNA and tested for recall after adoptive transfer (Fig. 7a). As shown in Fig. 7b-c, although $CD73^-$ MBCs transfected with LNP-GFP were not recalled as efficiently as the $CD73^+$

counterpart to produce GCs or PCs, LNP-Zfp318 transfection of CD73$^-$ MBCs led to a much stronger recall response giving rise to both GCs and PCs.

Abundance of Zfp318-expressing MBCs predicts the quality of vaccine-induced antibody responses.

Given the central role of Zfp318 in controlling the MBC recallability, strengths of antibody immunity induced by prime-boost vaccination should be predicted by the abundance of Zfp318-expressing GC-derived MBCs rather than the abundance of total MBCs. We validated this idea in three published settings of prime-boost vaccination. First, a colloidal manganese salt (Mn jelly, MnJ) is a superior adjuvant that, in part by activating cGAS-STING and NLRP3 pathways, promotes much stronger antibody responses as compared to what is achievable with alum as the adjuvant [28,29]. As shown in Fig. S9a-b, MnJ-adjuvanted immunization induced more ZFP318-expressing MBCs after the prime, whereas total antigen-binding MBCs were comparable to what was achieved with alum. Second, a tripartite fusion of the receptor-binding domain (RBD) of SARS-CoV2 S protein, type I interferon and immunoglobulin Fc domain (I-R-F) has been shown to be a superior vaccine candidate than alum-adjuvanted RBD, as demonstrated by much higher titers of total and neutralizing anti-RBD antibodies after the boost [30]. As shown in Fig. S9c-d, the I-R-F regimen induced more Zfp318-expressing RBD-specific MBCs as measured before the boost, whereas total RBD-binding MBCs were comparable between the two groups. Finally, we have previously compared two formulas of mRNA vaccines targeting the SARS-CoV2 RBD, one expressing the RBD dimmer and the other expressing trimerized RBD (3×RBD). The two formulas induced a very similar primary response in terms of GCs, PCs, total RBD-binding MBCs, and RBD-binding antibody titers, as measured right before the booster dose. After the boost, however, 3×RBD immunization led to a markedly higher titers of serum RBD-specific antibodies that persist long after the boost [31]. As shown in Fig. S9e-f, the abundance of Zfp318-expressing but not total RBD-binding MBCs, as measured before the boost, was much higher with 3×RBD than with RBD immunization. Taken together, these data support that Zfp318-expressing GC-derived MBCs, as the functionally dominant B cell memory component, are a better biomarker for durable humoral immunity.

Discussion

The issue of MBC recallability has not been appreciated before. By fate-mapping, cell deletion, gene ablation, inducible complementation and mRNA transfection experiments, we show that functional recall of B cell memory is predominantly determined by GC-derived MBCs and identify Zfp318 as the master regulator of the MBC recallability, being necessary and sufficient for the superior recall function of GC-derived MBCs. Zfp318 directly or indirectly control genes that mediate vital mitochondrial functions in MBCs. Given the contrast between Zfp318-deficient MBCs and naïve B cells, future studies are necessary to elucidate further how Zfp318 controls those mitochondrion-related genes and identify the co-factor(s) that contextualizes the cell type-specific gene regulation by Zfp318.

Our finding of differences in recallability between GC-dependent and -independent MBCs is in contrast to the previous report that Bcl-6-deficient MBCs, which could only develop from a GC-independent route, and Bcl-6-sufficient MBCs, which contain both GC-dependent and -independent cells, are comparably recalled to produce similar antibody responses in *Rag1*$^{-/-}$ mice [13]. While the precise reason for such a difference is not fully clear, we note that *Rag1*$^{-/-}$ mice and other lymphopenic hosts have abnormally high levels of BAFF [32,33]. BAFF is consumed by B cells in a competitive manner under physiological conditions [34]. When exuberantly present in lymphopenic animals, BAFF can rescue cells otherwise destined to die, such as self-reactive transitional B cells that recognize autoantigen but receive little T cell help [35,36]. As BAFF also promotes MBC longevity [37,38], we speculate that the exuberant BAFF in lymphopenic hosts can survive GC-independent MBCs that would otherwise die of re-activation-induced cell death.

Zfp318 expression is upregulated by CD40 but downregulated by BCR stimulation. Within the population of Zfp318-expressing GC-derived MBCs, the level of Zfp318 expression is positively correlated with BCR affinities. This observation suggests the graded ability to express Zfp318 is imprinted by T cell help. Interleukin 9, a cytokine that promotes MBC development from GCs [19], also promotes Zfp318 expression in GC memory precursor cells (unpublished observations). It appears that the more T-cell help MBCs receive during the course of development, the more likely and efficiently they can later survive activation-induced cell death and become productively recalled. When MBCs that actually participate in recall responses can be traced, they are found to be of comparatively high affinities and show significant clone overlap with MBCs giving rise to secondary PCs [39]. Human anti-smallpox MBCs that survive more than 40 years and can be reactivated *in vitro* have extensive GC experience and carry many affinity-enhancing mutations [16]. Persistent anti-SARS-CoV-2 MBCs are also GC-experienced and affinity-selected [14,15]. These observations are consistent with a functional recallability being dictated by prior experience of T cell help. GC-independent MBCs and GC-derived MBCs may represent two ends of a continuous spectrum of recallability dictated by Zfp318.

While functionally dominant, GC-derived MBCs represent a numerical minority in total antigen-binding MBCs following either protein immunization or viral infection, as shown here and elsewhere [4,5,12]. The large contingency of GC-independent MBCs might be recalled under special circumstances, for example, when exuberant T-cell help is available or when some innate stimuli could co-stimulate their recall. In this regard, it is notable that many viral infections cause increased BAFF production [40] and might thereby facilitate recruitment of otherwise hard-to-recall GC-independent MBCs to secondary responses. We propose that, by requiring T cell help for imprinting recallability of individual MBCs, the immune system may strike an appropriate balance between the need to exclude rogue clones from the readily recallable memory and from participating in the more long-lived humoral response and the need to maintain a memory repertoire of broad-spectrum specificities to deal with variants of mutating pathogens.

Acknowledgements

We thank Drs. B. Liu and T. Shao for critical comments of the manuscript. We thank Dr. M. Nussenzweig for providing the B1-8^{hi} mice. The work was funded in part by the National Key R&D Program of China (Ministry of Science and Technology, 2018YFE0200300 to H.Q.), National Natural Science Foundation of China (grant 31830023, 81621002 to H.Q., grant 31900629 to Y.W. and grant 32200725 to W.S.), the Changping Laboratory, the Tsinghua-Peking Center for Life Sciences, the Beijing Municipal Science & Technology Commission, and the Beijing Frontier Research Center for Biological Structure. H.Q. is a New Cornerstone Investigator.

Author contributions

H.Q. conceptualized and supervised the study. Y.W. and W.S. conducted a majority of the experiments. W.S. conducted RNA-seq analyses. X.L. made the initial design of the ZSDAT reporter. L.Y. advised EM studies. J.L. and G.Y. designed and prepared LNP. Q.L. helped with mRNA vaccine experiments under the supervision of L.Z. H.Q. wrote the paper with input from all authors.

Competing interest

Y.W. and H.Q. are co-founders of Emergent Biomed Solutions, Ltd.

Data availability

All data generated during and/or analyzed during the current study are available from the corresponding author upon reasonable request. Source data are included in this published article (and its supplementary information files).

Methods

Mice. C57BL/6 (Jax 664), GFP-transgenic (Jax 4353), AID-Cre (Jax 018422), Rosa26-Ai3 (Jax 7903), $OVA_{323–339}$-specific T-cell receptor transgenic OT-II (Jax 4194), Rosa26-CAGs-rtTA3 (Jax 029627), and CD45.1 (Jax 2014) mice were originally from the Jackson Laboratory. The ZFP318-reporting ZSDAT knock-in/knock-out strain mice were developed at BIOCYTOGEN by CRISPR/Cas9 technology. Ighd KO mice were developed at GemPharmatech by CRISPR/Cas9 technology. The B1-8^{hi} Ig heavy chain knock-in mice were a kind gift of Dr. M. Nussenzweig. All mice were maintained under specific pathogen-free conditions, and used in accordance of governmental and Tsinghua guidelines for animal welfare.

Immunization and viral infection. For immunization with SRBC, 1 ml SRBC suspension (Zhengzhou Baiji, Inc.) was intraperitoneally injected to each mouse. To measure the NP-specific response in various experiments, mice were intraperitoneally injected with 100 μg NP-KLH, 100 μg or 20 μg NP-OVA (Biosearch Technologies, 20 μg for recall) mixed with 2 μg LPS (Sigma) in alum (Thermo Scientific). To prepare carrier-primed mice for MBC transfer, mice were intraperitoneally immunized with 20 μg OVA mixed with 2 μg LPS in alum. For certain experiments, mice were intranasally infected with 50 PFU of PR8 influenza virus under anesthesia by intraperitoneal tribromoethanol (250 mg/kg), or intraperitoneally immunized with 50 μg hemagglutinin. To compare adjuvants, mice were intraperitoneally immunized with 100 μg NP-KLH mixed with lipopolysaccharide in alum or mixed with 300 μg MnJ (MnStarter Biotechnology), as previously described adjuvant[28,29]. To compare RBD and 3×RBD trimer mRNA vaccines, mice were intramuscularly immunized with 10 μg respective mRNA LNP. To compare recombinant RBD dimer or IFN-Pan-RBD-Fc vaccines, mice were subcutaneously immunized with 3.4 μg RBD dimer or 10.4 μg IFN-Pan-RBD-Fc protein, as previously described[30].

Flow cytometry. To profile different cell populations by flow cytometry, single-cell suspension was washed with PBS, and then stained with indicated antibodies in MACS buffer (PBS supplemented with 1% FBS and 5 mM EDTA). Staining reagents included PerCP Cy5.5 anti-IgD, PE-Cy7 anti-CD95, FITC anti-IgG3, PE anti-CD86, FITC anti-I-A/I-E from BD Biosciences; AF700 anti-CD38, EF450 anti-GL7, APC anti-CD80, APC anti-CD86, FITC anti-PD-L2 from eBioscience; allophycocyanin (APC)-Cy7 anti-B220, BV510 anti-CD138, FITC anti-IgG1, FITC anti-IgG2b, BV421 anti-IgM, PerCP Cy5.5 anti-Gr1, PE-CD73, APC-CCR6, streptavidin-APC, streptavidin-PE, MitoSpy™ NIR DiIC1(5) from Biolegend; FITC anti-IgG2c from Bethyl. Isotype-matched control antibodies were also purchased from these respective vendors. Surface staining was done on ice with primary reagents incubated for 30 minutes followed by secondary reagents for 30 minutes with washes in-between. To detect NP-binding cells in GC B cells, memory B cells, SPPCs or BMPCs, $NP_{(38)}$- or $NP_{(44)}$-PE or biotinylated $NIP_{(15)}$-BSA (Biosearch Technologies) were used. All cytometric data were collected on an LSR II, or an FACSAria III cytometer (BD Biosciences) or an Aurora cytometer (Cytek Biosciences) and analyzed with the FlowJo software (TreeStar). Dead cells and

non-singlet events were excluded from analyses based on staining with Zombie Yellow (Biolegend) and characteristics of forward and side scatters.

Recall assays of memory B cells. First, to measure the recall response by polyclonal memory B cells in a secondary host, *Zfp318*$^{+/ZSDAT}$AID-Cre mice were immunized and used as the donor of memory B cells 30 days after primary NP-KLH immunization. To isolate memory B cells, donor splenocytes were depleted of CD4^{+}, CD8^{+}, GL7^{+}, CD138^{+} and IgD^{+} cells using a cocktail of biotinylated anti-CD4, anti-CD8, anti-GL7, anti-CD138, anti-IgD antibodies in combination of streptavidin Microbeads (Miltenyi Biotec). CD19^{+} cells were then enriched using CD19 Microbeads (Miltenyi Biotec). The resulting memory B cell-enriched cell preparation was FACS-analyzed, normalized for the abundance of NIP-binding B220^{+}CD138^{-}GL7^{-}FAS^{-}CD38^{+}IgD^{-} memory B cells, and transferred into CD45.1 recipients that were primed with carrier protein OVA 30 days before. After cell transfer, these recipient mice were immunized with NP-OVA. To delete ZFP318-expressing cells, these mice were given 5 μg/kg diphtheria toxin or PBS intraperitoneally. The recall response by CD45.2^{+} donor-derived memory B cells was measured 7 days after NP-OVA immunization. Secondly, to measure the recall response by memory B cells carrying NP-specific BCRs in a secondary host, *Zfp318*$^{+/ZSDAT}$AID-Cre GFP-expressing B1-8^{hi} cells were adoptively transferred into B6 mice that also received OT-II T cells and were immunized with NP-OVA. Resulting NIP-binding B220^{+}CD138^{-}GL7^{-}FAS^{-}CD38^{+}IgD^{-}GFP^{+} memory B cells from these primary hosts were sort-purified into tdTomato^{+} and tdTomato^{-} cells, and these latter cells were transferred into separate groups of secondary B6 recipients that were primed with OVA protein 30 days before. These recipient mice were then immunized with NP-OVA, the recall response by GFP^{+} B1-8^{hi} memory B cells was measured 7 days after NP-OVA immunization. Third, to measure the recall response by ZFP318-deficient memory B cells, *Zfp318*$^{ZSDAT/ZSDAT}$AID-Cre Ai3 or control *Zfp318*$^{+/+}$AID-Cre Ai3 mice were immunized and used as the donor of memory B cells 30 days after primary NP-KLH immunization. To isolate memory B cells, donor splenocytes were depleted of CD4^{+}, CD8^{+}, GL7^{+}, and CD138^{+} cells using a cocktail of biotinylated anti-CD4, anti-CD8, anti-GL7, and anti-CD138 antibodies in combination of streptavidin Microbeads (Miltenyi Biotec). CD19^{+} cells were then enriched using CD19 Microbeads (Miltenyi Biotec). The resulting memory B cell-enriched cell preparation was FACS-analyzed, normalized for the abundance of NIP-binding B220^{+}CD138^{-}GL7^{-}FAS^{-}CD38^{+} memory B cells, and transferred into CD45.1 recipients that were primed with carrier protein OVA 30 days before. After cell transfer, these recipient mice were immunized with NP-OVA. The recall response by donor-derived memory B cells was measured 7 days after NP-OVA immunization. Fourth, to measure the recall response by by ZFP318-deficient memory B cells carrying NP-specific BCRs in a secondary host, *Zfp318*$^{+/ZSDAT}$AID-Cre GFP-expressing B1-8^{hi} cells or *Zfp318*$^{ZSDAT/ZSDAT}$AID-Cre GFP-expressing B1-8^{hi} cells were adoptively transferred into B6 mice that also received OT-II T cells and were immunized with NP-OVA. Resulting NIP-binding B220^{+}CD138^{-}GL7^{-}FAS^{-}CD38^{+}GFP^{+}tdTomato^{+} memory B cells from these primary hosts were sort-purified, and these cells were transferred into

separate groups of secondary B6 recipients that were primed with OVA protein 30 days before. These recipient mice were then immunized with NP-OVA, the recall response by GFP^+ B1-8^{hi} memory B cells was measured 7 days after NP-OVA immunization. For recalls with LNP, sorted MBCs were transfected with LNP carrying either Zfp318 or GFP mRNAs (1 μg RNA/10^5 cells) and incubated in RPMI at 37°C for 3 hrs. Cells were then washed by PBS, and prepared for adoptive transfer.

Encapsulation of RNA by LNP. LNP was fabricated by extruding two phases (aqueous phase and ethanol phase). Ethanol phase: The cationic lipid, cholesterol, PEG-lipid, and DSPE were used as the lipid phase to fabricate LNP. The four components were dissolved into pure ethanol. To facilitate dissolution, the solution was slightly heated by a heat gun (hair dryer) before using. DSPE and PEG-lipid would separate from ethanol solution at 4 ℃. The concentration of the cationic lipid, cholesterol, PEG-lipid, and DSPE is 43 mg/ml, 20 mg/ml, 10 mg/ml, and 9 mg/ml, respectively. The volume of cationic lipid, cholesterol, PEG-lipid, and DSPE is 100 μl, 100 μl, 50 μl, and 100 μl, respectively. After adding the four components together, 100 μl ethanol was added. The final volume of ethanol was 450 μl. Aqueous phase: RNA was dissolved into 50mM citrate buffer with a concentration of 100 μg/900 μl. After loading the two phases into corresponding syringes, the two syringes were extruded with the speed ratio 1:3 (ethanol phase: buffer phase). The extruded LNP was dialyzed against PBS for 2 hours and water for 3 hours. After the dialyzation process, to check the quality of LNP, the diameter, polydispersity index, zeta potential of LNP were tested by Zetasizer Nano (Malvern Instruments, Malvern, UK) at least 5 times. All experiments were carried out using freshly packaged LNP within 12 h.

V_H186.2 sequence analysis of NP-specific B cells. NP-specific memory B cells were identified by staining with biotinylated $NIP_{(15)}$-BSA (Biosearch Technologies) at 330 ng/ml for 30 min on ice and then with streptavidin APC. NIP-binding $GL7^-FAS^-$ $B220^+CD138^-IgD^-CD38^+$ memory B cells were sort-purified 14 or 28 days after NP-KLH immunization. After incubation at 60 °C for 5 min in the lysis buffer, lysates of multiple 200-cell sorts per experiment was subjected to reverse-transcription by with the Superscript cDNA Synthesis Kit (Invitrogen) using the manufacturer's suggested protocol. V_H186.2 fragments were amplified from the complementary DNA by nested PCR using the following primers (first and second sense: 5′-TTCTTGGCAGCAACAGCTACA, first antisense including Cγ1 antisense: 5′-GGATCCAGAGTTCCAGGTCACT and Cμ antisense 5′-AAATGGTGCTGGGCAGGAAG; second antisense including Cγ1 antisense: 5′-GGAGTTAGTTTGGGCAGCAG and Cμ antisense 5′-AGCCCATGGCCACCAGATT). PCR products were purified by gel electrophoresis and cloned into a T vector (Takara), and individual bacterial colonies were picked for sequencing. Identical V_H sequences were counted only once as one clone, and the final result was compiled with unique clones for each category.

Quantitative RT-PCR. Quantitative RT-PCR was performed with a SYBR *Premix Ex*

Taq II (Tli RNaseH Plus) (RR820; Takara) on a 7500 Real-Time PCR system (Thermo Fisher). Primers used were: *Actb* sense 5′-GCTTCTTTGCAGCTCCTT, antisense 5′-TGCCAGATCTTCTCCATGT; *Zfp318* sense 5′- ATGTGAGCCCTCGGGAAATG, antisense 5′-TGCCGGTTCCAGATGAGATT. *Dtr* sense 5′-AGGGAAGAAGAGGGACCCAT, antisense 5′- AACATGAGAAGCCCCACGAT.

Measurement of serum NP-specific IgG by ELISA. Sera were harvested from relevant mice and stored at -80°C until use. 96-well ELISA plates (42592, Costar) were coated with NP_{23}-BSA (Biosearch Technologies) in PBS overnight and washed. A serial 1:2 dilution of each serum sample, starting from 1:800, was then loaded into the plate and incubated at 37 °C for 1 h. After washings, the plate was further incubated with HRP-conjugated goat anti-mouse IgG (poly4053, Biolegend) at 1:20,000 for 1 h before development with TMB Substrate Set (421101, Biolegend). The chromogenic reaction was stopped with 1 M HCL, and optical density (OD) was read on an iMark plate reader. For each group of animals, the resulting dilution curves were fit with the 3-parameter dose–response curve in Prism (Graphpad). Curves from two groups in comparison were analyzed by the extra sum-of-squares F-test, and their nominal EC50s were used to calculate fold-change in NP-specific IgG titers.

Electron Microscopy. Sort-purified memory B cells or naïve B cells were fixed with 2.5% glutaraldehyde in 0.1M PB buffer for 2 h and then rinsed 3× 10 min with the PB buffer. Post-fixation staining was performed with 1% osmium tetroxide/$K_3Fe(CN)_6$ for 30 min. After washing in distilled water 3× 5 min, cells were dehydrated in a graded ethanol series (50%, 70%, 80%, 90%, 100%, 100%) for 5 min each. After the final incubation in 100% ethanol at the room temperature, cells were incubated in a 1:1 mix of ethanol and acetone for 5 min and then in 100% acetone for 5 min. Cells were then infiltrated and embedded in Pon 812 resin. The blocks were trimmed, and 70-nm sections were contrast-stained with uranyl acetate and citrate. Cells were then examined with TEM (Hitachi, H7650). Numbers of mitochondria per cell section, fractional mitochondrion-occupied area, and mitochondria density were quantitated with imageJ.

RNA-seq and data analysis. Approximately 200-1000 cells of desired type were lysed in 6 µl lysis buffer (0.2% Triton X-100 and 2 U/µl of RNase inhibitor). Lysates were mixed with 3 µl of anchored oligo-dT primer (10 µM, 5′-AAGCAGTGGTATCAACGCAGAGTACT30VN-3′) and 3 µl of dNTP mix (10 mM, Fermentas), denatured at 72 °C for 3 min and immediately placed on ice afterwards. The first-strand reaction mix containing 1 µl SuperScript II reverse transcriptase (Invitrogen), 0.5 µl RNAse inhibitor (Clontech), 4 µl Superscript II First-Strand Buffer (Invitrogen), 1 µl DTT (100 mM, Invitrogen), 4 µl betaine (5 M, Sigma), 0.12 µl $MgCl_2$ (1 M, Sigma), 0.2 µl TSO (100 µM) and 0.58 µl nuclease-free water, were added to each sample. Reverse transcription reaction was carried out by incubating at 42 °C for 90 min, followed by 10 cycles of (50 °C for 2 min, 42 °C for 2 min). Finally, the reverse transcriptase was inactivated by incubation at 70 °C for 15 min. PCR mix containing

25 μl KAPA HiFi HotStart ReadyMix, 0.5 μl IS PCR primers (10 μM) and 1.1 μl nuclease-free water were added to each sample. The reaction was incubated at 98 °C for 3 min, then cycled 17 times (98 °C 20 s, 67 °C 15 s, 72 °C 6 min), with a final extension at 72 °C for 5 min. cDNAs were purified by Vazyme DNA clean beads following manufacturer's instructions. 1 ng of cDNA were used for the tagmentation reaction using Tn5 (Vazyme). The tagmentation reaction (20 μl) was incubated at 55 °C for 10 min and stopped by addition of 2 μl 0.2%SDS and incubated at 70 °C for 20 min. A second amplification was performed using Q5 polymerase (NEB) as follows: 72 °C 3 min, 98 °C 30 s, then 12 cycles of (98 °C 15 s, 60 °C 30 s, 72 °C 3 min), final extension at 72 °C 5 min. Libraries were purified using Vazyme DNA clean beads. The clean reads were mapped to the mouse genome (mm10) through STAR v2.2.0 with default settings. FeatureCounts software was used to collect reads located in the coding sequence (CDS) of each gene. CDS counts normalized to mappable reads were used for measuring gene expression. To compare gene expression between Zfp318-deficient and Zfp318-expressing MBCs across three different experimental settings, z-score of each gene was firstly calculated within each dataset to preclude batch and background bias, and then k-means clustering analysis was conducted using R software (v4.0.2). Gene set analysis was performed using GSEA software (v4.1.0). Expression profiles of all genes in the three settings were used as the input dataset and gene set c5.go.bp.v2023.1.Hs.symbols.gmt was used for enrichment analysis.

Experimental grouping and statistical data analyses. For all relevant animal experiments, age- and sex-matched mice were randomly chosen to be included in different treatment groups. Each group typically had 3 to 5 animals, and 2 to 6 independent experiments were conducted for every assay. No blinding was necessary for animal experiments involved in this work. Except when noted otherwise, two-tailed Student's *t* tests were used to compare endpoint means of different groups. Graphs were made in Prism (GraphPad).

Figure legends

Figure 1. MBC heterogeneity revealed by the ZSDAT reporter.
a, Representative tdTomato fluorescence profiles of GCs, MBCs, splenic PCs, and bone-marrow PCs from AID-Cre (top row) or *Zfp318*$^{ZSDAT/+}$AID-Cre mice (bottom row) 14 days after NP-KLH immunization. **b**, Frequencies of tdTomato^{+} cells in GCs, MBCs, splenic PCs, and BMPCs observed 14, 28 or 64 days after NP-KLH immunization. Data pooled from 2 independent experiments. *P* values by one-way ANOVA. **c**-**d**, Representative FACS profiles of EYFP (Rosa26-Ai3) and tdTomato (ZSDAT) fluorescence (**c**) and summary data (**d**) of MBCs AID-Cre;*Zfp318*$^{ZSDAT/+}$;Rosa26-Ai3 mice treated with PBS (left) or DT (right) for 24 hours that are 60 days after NP-KLH immunization. **e**, Overall mutations (mean±s.e.m.) per V_H186.2 heavy chain and frequencies of affinity-enhancing W33L mutations in tdTomato^{+} or tdTomato^{-} NP-binding MBCs sorted from AID-Cre;*Zfp318*$^{ZSDAT/+}$ mice 14 or 28 days after immunization. Numbers of analyzed clones are indicated at the center of the pie chart. Data are pooled from 2 independent experiments, involving >10 mice per group. *P* values by *t* tests (top, overall mutations) and by Fisher's exact test (bottom, W33L mutations).

Figure 2. Recallable memory is carried in Zfp318-expressing MBCs.
Recall in CD45.1 recipients of MBCs from AID-Cre;*Zfp318*$^{ZSDAT/+}$ mice. **a**, Experimental design. **b**-**c**, Gating strategy to identify donor-derived cells (**b**) and summary data (**c**) of donor-derived GCs, splenic PCs, in PBS- or DT-treated group 7 days after re-challenge, as done according to (**a**). Data were pooled from 4 independent experiments, with each symbol indicating one mouse and lines denoting means. *P* values by *t* tests.

Figure 3. Zfp318 underlies MBC recallability.
a, Experimental design. **b**, Gating strategies to identify GCs and SPPCs. **c**, Gating strategies to identify GFP^{+} (Ai3 reporter) GCs and SPPCs. **d**, Summary data of cell abundance of indicated types. Data were pooled from 2 independent experiments, with each symbol indicating one mouse and lines denoting means. *P* values by Mann-Whitney tests.

Figure 4. Induction of Zfp318 leads to recall rescue.
a, Diagrams of *Col1a1*$^{Teton\text{-}zfp318}$ and *Rosa26*$^{LSL\text{-}rtTA3}$ alleles. **b**, Experimental design. **c**, The gating strategy to sort-purify CD73^{+} and CD73^{-} B1-8^{hi} MBCs. **d**, Zfp318 expression in CD73^{+} and CD73^{-} B1-8^{hi} MBCs by qPCR. *P* values by Student's *t* tests. **e-f,** Gating strategy to identify donor-derived cells (**e**) and summary data (**f**) of GCs and splenic PCs derived from control CD73^{-}, Zfp318-induced CD73^{-} and control CD73^{+} B1-8^{hi} MBCs 7 days after recall. Data were pooled from 2 independent experiments, with each symbol indicating one mouse and lines denoting means. *P* values by Mann-Whitney tests.

Figure 5. Zfp318 expression is promoted by CD40 signaling and correlated with antigen-binding affinities.
a-b, *Zfp318* mRNA levels in naïve B cells, DZ GC B cells, or LZ GC B cells after 4-hour stimulation with anti-IgM/IgG (**a**), anti-CD40 (**b**) or respective controls (**a-b**). Data were pooled from 5 independent experiments with each pair of circles indicating one experiment. *P* values by paired *t* tests. **c-d**, Scatter plots of tdTomato mean fluorescence intensities (MFI) versus relative affinities of individual antigen-binding MBCs (calculated as antigen-binding MFI divided by IgM or IgG MFI), measured in AID-Cre;*Zfp318*$^{ZSDAT/+}$ mice 14 days after NP-KLH immunization for NIP-binding MBCs (**c**) or 10 days after PR8 infection for HA-binding MBCs (**d**). Linear regression lines are shown, and *P* values for correlation are by linear regression tests. Individual dots are individual cells.

Figure 6. Zfp318 orchestrates a mitochondrial state conducive to recall.
a-f, Transcriptomic features of Zfp318-expressing (Zfp318^{+}) MBCs compared to Zfp318-deficient (Zfp318^{-}) MBCs. **a-c**, Three experimental settings. **d**, K-means clustering analysis of differentially expressed genes (P<0.05 at least in one experimental setting) pooled from the 3 experimental settings comparing Zfp318^{+} and Zfp318^{-} MBCs. **e,** Gene ontology analysis of genes up-regulated in Zfp318^{+} compared to Zfp318^{-} MBCs (P<10^{-5}). **f**, GSEA analysis showing enrichment of mitochondrion-related pathways (P<0.05). Normalized enrichment score (NES), *p* values, and FDR are given in the graphs. **g,** Histogram overlay of mitoSpy fluorescence of Zfp318^{+} and Zfp318^{-} MBCs in the 3 different experimental settings (**a-c**). **h-k**, Electron microscopy of sort-purified B1-8^{hi} MBCs. **h**, Representative micrographs of sort-purified B1-8^{hi} MBCs of indicated types. Blue arrow indicates normal mitochondrion, and red arrow indicates compromised one. **i**, Nominal numbers (Left) and fractional areas (Right) of mitochondria in MBCs and naïve B cells (also see Fig. S8), quantitated from micrographs as in (**h**). Each symbol represent one cell, and lines denote means. Data were pooled from 2 independent experiments. *P* values by *t* tests. **j**, Representative micrographs of cristae morphology in mitochondria. **k**, Fractional abundance of structurally compromised mitochondria in tdTomato^{+} MBCs. *P* values by Fisher's exact tests. **l**, Representative profiles of cleaved caspase-3 expression by tdTomato^{+} B1-8^{hi} MBCs of an AID-Cre;*Zfp318*$^{ZSDAT/+}$ or AID-Cre;*Zfp318*$^{ZSDAT/ZSDAT}$ genotype, which were untreated or stimulated with an anti-IgM/G antibody (10 μg/ml) for 3 h. **m**, Representative profiles of cleaved caspase-3 expression by tdTomato^{+} B1-8^{hi} MBCs of an AID-Cre;*Zfp318*$^{ZSDAT/ZSDAT}$;*Col1a*$^{TetOn\text{-}Zfp318/+}$;*Rosa*$^{LSL\text{-}rtTA3}$ or AID-Cre;*Zfp318*$^{ZSDAT/ZSDAT}$;*Col1a*$^{+/+}$;*Rosa*$^{LSL\text{-}rtTA3}$ genotype, which were untreated or stimulated with an anti-IgM/G antibody (10 μg/ml) for 3 h.

Figure 7. Reprogramming recallability by exogenous Zfp318.
a, Recall experiments using sorted CD73^{+} or CD73^{-} MBCs that were transfected with LNP carrying control GFP or Zfp318 mRNAs. **b-c**, Gating strategy to identify donor-

derived cells (**b**) and summary data (**c**) of GCs and splenic PCs derived from control CD73$^-$, Zfp318-induced CD73$^-$ and control CD73$^+$ MBCs 7 days after recall. Data were pooled from 2 independent experiments, with each symbol indicating one mouse and lines denoting means. *P* values by Mann-Whitney tests.

Figure S1. Validation of the ZSDAT reporter.
a-b, Zfp318 expression by B cells. **a,** The gating strategy for sorting CD38$^+$ GC memory precursors (top row), memory B cells (middle row), and plasma cells (bottom row). **b,** Zfp318 mRNA levels by quantitative RT-PCR in sort-purified B cells 8 days after SRBC immunization (RQ: *Actin* as reference). Shown are mean±s.e.m. of triplicated wells from one of 3 experiments with similar results. **c**, The diagram of ZSDAT reporter allele. STOP, transcription stop cassette; black triangles, flox sites. **d-e**, Zfp318 (**d**) and corresponding DTR mRNA levels (**e**) by quantitative RT-PCR in tdTomato$^+$ or tdTomato$^-$ cells of indicated types (GFP-expressing *Zfp318*$^{ZSDAT/+}$;AID-Cre B1-8^{hi} cells in B6 mice 7 days after NP-OVA immunization). **f**, Normalized abundance of the tdTomato$^+$ fraction in MBCs from NP-KLH-immunized *Zfp318*$^{ZSDAT/+}$;AID-Cre mice, at indicated time points after DT treatment. Data were pooled from 4 independent experiments. In each, the mean value of the PBS group is set as unit 1.

Figure S2. Loss of one functional *Zfp318* allele does not impair the primary response.
a-c, FACS profiles (**a**) and summary data (**b**) of GCs, SPPCs, BMPCs, serum NP_7- and NP_{30}-binding antibodies (**c**) in AID-Cre;*Zfp318*$^{+/+}$ or AID-Cre;*Zfp318*$^{ZSDAT/+}$ mice on day 28 after NP-KLH immunization. In all scatter plots, each symbol is one mouse, and lines denote means. Data are pooled from 2 independent experiments. *P* values by *t* tests.

Figure S3. Zfp318 is not required for the primary B cell response.
a-c, FACS profiles (**a**) and summary data (**b**) of GCs, SPPCs, BMPCs, serum anti-NP antibodies (**c**) in AID-Cre;*Zfp318*$^{+/+}$ or AID-Cre;*Zfp318*$^{ZSDAT/ZSDAT}$ mice on day 28 after NP-KLH immunization. In all scatter plots, each symbol is one mouse, and lines denote means. Data are pooled from 3 independent experiments.

Figure S4. Zfp318-expressing MBCs are responsible for GC-dependent recall.
a, Recall experiments using MBCs from AID-Cre;*Zfp318*$^{ZSDAT/+}$ mice. **b-c**, Gating strategy to identify donor-derived cells (**b**) and summary data (**c**) of donor GCs and SPPCs in PBS- or DT-treated group 7 days after HA immunization, as done according to (**a**). Data were pooled from 2 independent experiments, with each symbol indicating one mouse and lines denoting means. *P* values by Mann-Whitney tests.

Figure S5. IgD is not required for MBC recall.

a, Experimental design of recall experiments utilizing MBCs from *Ighd*$^{+/+}$ and *Ighd*$^{-/-}$ mice. **b-c**, Representative FACS profiles (**b**) and summary data (**c**) of GCs and splenic PCs 7 days after re-challenge, as done according to (**a**). Each symbol indicating one mouse and lines denoting means. *P* values by *t* tests.

Figure S6. Zfp318 underlies MBC recallability.
a-c, Recall experiments utilizing adoptive transfer of GFP-expressing AID-Cre;*Zfp318*$^{ZSDAT/+}$ or AID-Cre;*Zfp318*$^{ZSDAT/ZSDAT}$ B1-8^{hi} cells isolated on day 30 after immunization. **a**, Experimental design. Top 30% tdTomato-expressing MBCs were sort-purified for the transfer. **b-c**, Gating strategy to identify donor-derived cells (**b**) and summary data (**c**) of GCs and splenic PCs derived from *Zfp318*$^{ZSDAT/+}$ and *Zfp318*$^{ZSDAT/ ZSDAT}$ B1-8^{hi} MBCs 7 days after recall, as done according to (**a**). Data were pooled from 2 independent experiments, with each symbol indicating one mouse and lines denoting means. *P* values by Mann-Whitney *t* tests. **d-g**, Recall experiments utilizing adoptive transfer of GFP-expressing AID-Cre;*Zfp318*$^{ZSDAT/+}$ or AID-Cre;*Zfp318*$^{ZSDAT/ZSDAT}$ B1-8^{hi} cells isolated on day 7 after immunization. **d**, Experimental design. **e**, The gating strategy to sort-purify tdTomato^{+} B1-8^{hi} MBCs. Left, an overlay of GCs and MBCs to show their difference in tdTomato fluorescence. Right, tdTomato^{+} gate for MBCs. **f-g**, Gating strategy to identify donor-derived cells (**f**) and summary data (**g**) of GCs and splenic PCs derived from *Zfp318*$^{ZSDAT/+}$ and *Zfp318*$^{ZSDAT/ ZSDAT}$ B1-8^{hi} MBCs 7 days after recall. Data were pooled from 2 independent experiments, with each symbol indicating one mouse and lines denoting means. *P* values by Mann-Whitney tests.

Figure S7. CD73^{+} MBCs are enriched with Zfp318-expressing MBCs.
a, CD73 expression of tdTomato^{+} MBCs or tdTomato^{-} MBCs 28 days after NP-KLH immunization. **b**, TdTomato expression of CD73^{+} MBCs or CD73^{-} MBCs 28 days after NP-KLH immunization. **c-e**, Recall experiments utilizing MBCs from B6 mice. **c**, Experimental design. **d-e**, Gating strategy to identify donor-derived cells (**d**) and summary data (**e**) of GCs and SPPCs derived from CD73^{+} and CD73^{-} MBCs. Data were pooled from 2 independent experiments, with each symbol indicating one mouse and lines denoting means. *P* values by *t* tests.

Figure S8. Zfp318 orchestrates a mitochondrial state conducive to recall.

a-b, Transcriptomic features of Zfp318-sufficient (Zfp318^{+}) MBCs compared to Zfp318-deficient (Zfp318^{-}) MBCs. **a**, K-means clustering analysis of differentially expressed genes (P<0.05 at least in one experimental setting) pooled from 3 experimental settings (see Fig. 6a-c) between Zfp318^{+} and Zfp318^{-} MBCs, identifying 12 clusters. **b**, Gene ontology analysis of genes down-regulated in Zfp318^{+} (cluster B) compared to Zfp318^{-} MBCs (P<10^{-5}). **c**, Heatmap of mitochondrial translation genes that are upregulated in Zfp318^{+} MBCs compared to Zfp318^{-} MBCs. **d,** Heatmap of genes involved in ATP synthesis that are upregulated in Zfp318^{+} MBCs compared to Zfp318^{-} MBCs. **e**, GSEA showing enrichment of cellular oxidant detoxification

pathway in Zfp318^{+} compared to Zfp318^{-} MBCs. Normalized enrichment score (NES), *p* values, gene numbers and FDR are given in the graphs. **f**, Heatmap showing genes involved in cellular oxidant detoxification that are upregulated in Zfp318^{+} MBCs compared to Zfp318^{-} MBCs. **g**, Heatmap showing genes involved in negative regulation of release of cytochrome c from mitochondria that are upregulated in Zfp318^{+} MBCs compared to Zfp318^{-} MBCs. **h**, Representative micrographs of sort-purified B1-8^{hi} naïve B cells of indicated types.

Figure S9. The abundance of Zfp318-expressing MBCs predicts the quality of prime-boost vaccination.

a-b, Comparison between two adjuvants. **a**, Representative profiles of tdTomato fluorescence of MBCs 14 days after NP-KLH immunization adjuvanted with alum and LPS or MnJ, in *Zfp318*$^{ZSDAT/+}$;AID-Cre mice. **b**, Summary data of total MBCs as a fraction of splenic B cells or tdTomato^{+} MBCs as a fraction of total MBCs. Each symbol is one mouse, and lines denote means. Data are pooled from 4 independent experiments. **c-d**, Comparison between two recombinant vaccine formula. **c**, Representative profiles of tdTomato fluorescence of MBCs 14 days after immunization with a SARS-CoV2 RBD dimer or an IFN-RBD-Fc fusion, in *Zfp318*$^{ZSDAT/+}$;AID-Cre mice. **d**, Summary data of total MBCs as a fraction of splenic B cells or tdTomato^{+} MBCs as a fraction of total MBCs. Each symbol is one mouse, and lines denote means. Data are pooled from 2 independent experiments. **e-f**, Comparison between two mRNA vaccine formula. **e**, Representative profiles of tdTomato fluorescence of MBCs 21 days after immunization with mRNA vaccine expressing SARS-CoV2 RBD or SARS-CoV2 RBD trimer (3×RBD), in *Zfp318*$^{ZSDAT/+}$;AID-Cre mice. **f**, Summary data of total MBCs as a fraction of splenic B cells or tdTomato^{+} MBCs as a fraction of total MBCs. Each symbol is one mouse, and lines denote means. Data are pooled from 4 independent experiments. *P* values by *t* tests.

References

1. Weisel, F., and Shlomchik, M. (2017). Memory B Cells of Mice and Humans. Annual Review of Immunology *35*, 255–284. 10.1146/annurev-immunol-041015-055531.

2. Tarlinton, D., and Good-Jacobson, K. (2013). Diversity Among Memory B Cells: Origin, Consequences, and Utility. Science *341*, 1205–1211. 10.1126/science.1241146.

3. Kurosaki, T., Kometani, K., and Ise, W. (2015). Memory B cells. Nature Reviews Immunology *15*, 149–159. 10.1038/nri3802.

4. Dogan, I., Bertocci, B., Vilmont, V., Delbos, F., Mégret, J., Storck, S., Reynaud, C.-A., and Weill, J.-C. (2009). Multiple layers of B cell memory with different effector functions. Nat Immunol *10*, 1292–1299. 10.1038/ni.1814.

5. Pape, K.A., Taylor, J.J., Maul, R.W., Gearhart, P.J., and Jenkins, M.K. (2011). Different B Cell Populations Mediate Early and Late Memory During an Endogenous Immune Response. Science *331*, 1203–1207. 10.1126/science.1201730.

6. McHeyzer-Williams, L.J., Milpied, P.J., Okitsu, S.L., and McHeyzer-Williams, M.G. (2015). Class-switched memory B cells remodel BCRs within secondary germinal centers. Nat Immunol *16*, 296–305. 10.1038/ni.3095.

7. Zuccarino-Catania, G.V., Sadanand, S., Weisel, F.J., Tomayko, M.M., Meng, H., Kleinstein, S.H., Good-Jacobson, K.L., and Shlomchik, M.J. (2014). CD80 and PD-L2 define functionally distinct memory B cell subsets that are independent of antibody isotype. Nature Immunology *15*, 631–637. 10.1038/ni.2914.

8. Burton, D.R., Ahmed, R., Barouch, D.H., Butera, S.T., Crotty, S., Godzik, A., Kaufmann, D.E., McElrath, J.M., Nussenzweig, M.C., Pulendran, B., et al. (2012). A Blueprint for HIV Vaccine Discovery. Cell Host & Microbe *12*. 10.1016/j.chom.2012.09.008.

9. Corti, D., and Lanzavecchia, A. (2013). Broadly Neutralizing Antiviral Antibodies. Immunology *31*, 705–742. 10.1146/annurev-immunol-032712-095916.

10. Toyama, H., Okada, S., Hatano, M., Takahashi, Y., Takeda, N., Ichii, H., Takemori, T., Kuroda, Y., and Tokuhisa, T. (2002). Memory B Cells without Somatic Hypermutation Are Generated from Bcl6-Deficient B Cells. Immunity *17*, 329–339. 10.1016/s1074-7613(02)00387-4.

11. Takemori, T., Kaji, T., Takahashi, Y., Shimoda, M., and Rajewsky, K. (2014). Generation of memory B cells inside and outside germinal centers. European Journal of Immunology *44*, 1258–1264. 10.1002/eji.201343716.

12. Taylor, J.J., Pape, K.A., and Jenkins, M.K. (2012). A germinal center–independent pathway generates unswitched memory B cells early in the primary response. J Exp Med *209*, 597–606. 10.1084/jem.20111696.

13. Kaji, T., Ishige, A., Hikida, M., Taka, J., Hijikata, A., Kubo, M., Nagashima, T., Takahashi, Y., Kurosaki, T., Okada, M., et al. (2012). Distinct cellular pathways select germline-encoded and somatically mutated antibodies into immunological memory. J Exp Med *209*, 2079–2097. 10.1084/jem.20120127.

14. Sokal, A., Chappert, P., Barba-Spaeth, G., Roeser, A., Fourati, S., Azzaoui, I., Vandenberghe, A., Fernandez, I., Meola, A., Bouvier-Alias, M., et al. (2021). Maturation and persistence of the anti-SARS-CoV-2 memory B cell response. Cell *184*, 1201-1213.e14. 10.1016/j.cell.2021.01.050.

15. Burton, A.R., Guillaume, S.M., Foster, W.S., Wheatley, A.K., Hill, D.L., Carr, E.J., and Linterman, M.A. (2022). The memory B cell response to influenza vaccination is impaired in older persons. Cell Reports *41*, 111613. 10.1016/j.celrep.2022.111613.

16. Chappert, P., Huetz, F., Espinasse, M.-A., Chatonnet, F., Pannetier, L., Silva, L.D., Goetz, C., Mégret, J., Sokal, A., Crickx, E., et al. (2022). Human anti-smallpox long-lived memory B cells are defined by dynamic interactions in the splenic niche and long-lasting germinal center imprinting. Immunity *55*, 1872-1890.e9. 10.1016/j.immuni.2022.08.019.

17. Laidlaw, B.J., Schmidt, T.H., Green, J.A., Allen, C.D.C., Okada, T., and Cyster, J.G. (2017). The Eph-related tyrosine kinase ligand Ephrin-B1 marks germinal center and memory precursor B cells. J Exp Medicine *214*, 639–649. 10.1084/jem.20161461.

18. Suan, D., Kräutler, N.J., Maag, J.L.V., Butt, D., Bourne, K., Hermes, J.R., Avery, D.T., Young, C., Statham, A., Elliott, M., et al. (2017). CCR6 Defines Memory B Cell Precursors in Mouse and Human Germinal Centers, Revealing Light-Zone Location and Predominant Low Antigen Affinity. Immunity *47*, 1142-1153.e4. 10.1016/j.immuni.2017.11.022.

19. Wang, Y., Shi, J., Yan, J., Xiao, Z., Hou, X., Lu, P., Hou, S., Mao, T., Liu, W., Ma, Y., et al. (2017). Germinal-center development of memory B cells driven by IL-9 from follicular helper T cells. Nature immunology *18*, 921–930. 10.1038/ni.3788.

20. Ishizuka, M., Ohtsuka, E., Inoue, A., Odaka, M., Ohshima, H., Tamura, N., Yoshida, K., Sako, N., Baba, T., Kashiwabara, S., et al. (2016). Abnormal spermatogenesis and male infertility in testicular zinc finger protein Zfp318-knockout mice. Dev Growth Differ *58*, 600–608. 10.1111/dgd.12301.

21. Enders, A., Short, A., Miosge, L.A., Bergmann, H., Sontani, Y., Bertram, E.M., Whittle, B., Balakishnan, B., Yoshida, K., Sjollema, G., et al. (2014). Zinc-finger protein ZFP318 is essential for expression of IgD, the alternatively spliced Igh product made by mature B lymphocytes. Proc National Acad Sci *111*, 4513–4518. 10.1073/pnas.1402739111.

22. Pioli, P.D., Debnath, I., Weis, J.J., and Weis, J.H. (2014). Zfp318 Regulates IgD Expression by Abrogating Transcription Termination within the Ighm/Ighd Locus. J Immunol *193*, 2546–2553. 10.4049/jimmunol.1401275.

23. Roes, J., and Rajewsky, K. (1993). Immunoglobulin D (IgD)-deficient mice reveal an auxiliary receptor function for IgD in antigen-mediated recruitment of B cells. J Exp Medicine *177*, 45–55. 10.1084/jem.177.1.45.

24. Akkaya, M., Kwak, K., and Pierce, S.K. (2020). B cell memory: building two walls of protection against pathogens. Nat Rev Immunol *20*, 229–238. 10.1038/s41577-019-0244-2.

25. Elgueta, R., Marks, E., Nowak, E., Menezes, S., Benson, M., Raman, V.S., Ortiz, C., O'Connell, S., Hess, H., Lord, G.M., et al. (2015). CCR6-Dependent Positioning of Memory B Cells Is Essential for Their Ability To Mount a Recall Response to Antigen. J Immunol *194*, 505–513. 10.4049/jimmunol.1401553.

26. Akkaya, M., Traba, J., Roesler, A.S., Miozzo, P., Akkaya, B., Theall, B.P., Sohn, H., Pena, M., Smelkinson, M., Kabat, J., et al. (2018). Second signals rescue B cells from activation-induced mitochondrial dysfunction and death. Nat Immunol *19*, 871–884. 10.1038/s41590-018-0156-5.

27. Purtha, W.E., Tedder, T.F., Johnson, S., Bhattacharya, D., and Diamond, M.S. (2011). Memory B cells, but not long-lived plasma cells, possess antigen specificities for viral escape mutants. J Exp Med *208*, 2599–2606. 10.1084/jem.20110740.

28. Zhang, R., Wang, C., Guan, Y., Wei, X., Sha, M., Yi, M., Jing, M., Lv, M., Guo, W., Xu, J., et al. (2021). Manganese salts function as potent adjuvants. Cell Mol Immunol *18*, 1222–1234. 10.1038/s41423-021-00669-w.

29. Wang, C., Guan, Y., Lv, M., Zhang, R., Guo, Z., Wei, X., Du, X., Yang, J., Li, T., Wan, Y., et al. (2018). Manganese Increases the Sensitivity of the cGAS-STING Pathway for Double-Stranded DNA and Is Required for the Host Defense against DNA Viruses. Immunity *48*, 675-687.e7. 10.1016/j.immuni.2018.03.017.

30. Sun, S., Cai, Y., Song, T.-Z., Pu, Y., Cheng, L., Xu, H., Sun, J., Meng, C., Lin, Y., Huang, H., et al. (2021). Interferon-armed RBD dimer enhances the immunogenicity of RBD for sterilizing immunity against SARS-CoV-2. Cell Res, 1–13. 10.1038/s41422-021-00531-8.

31. Liang, Q., Wang, Y., Zhang, S., Sun, J., Sun, W., Li, J., Liu, Y., Li, M., Cheng, L., Jiang, Y., et al. (2022). RBD trimer mRNA vaccine elicits broad and protective immune responses against SARS-CoV-2 variants. Iscience *25*, 104043. 10.1016/j.isci.2022.104043.

32. Cassani, B., Poliani, P.L., Marrella, V., Schena, F., Sauer, A.V., Ravanini, M., Strina, D., Busse, C.E., Regenass, S., Wardemann, H., et al. (2010). Homeostatic expansion of autoreactive immunoglobulin-secreting cells in the Rag2 mouse model of Omenn syndrome. J Exp Med *207*, 1525–1540. 10.1084/jem.20091928.

33. Walter, J.E., Rucci, F., Patrizi, L., Recher, M., Regenass, S., Paganini, T., Keszei, M., Pessach, I., Lang, P.A., Poliani, P.L., et al. (2010). Expansion of immunoglobulin-secreting cells and defects in B cell tolerance in Rag-dependent immunodeficiency. J Exp Med *207*, 1541–1554. 10.1084/jem.20091927.

34. Harless, S.M., Lentz, V.M., Sah, A.P., Hsu, B.L., Clise-Dwyer, K., Hilbert, D.M., Hayes, C.E., and Cancro, M.P. (2001). Competition for BLyS-mediated signaling through Bcmd/BR3 regulates peripheral B lymphocyte numbers. Curr Biol *11*, 1986–1989. 10.1016/s0960-9822(01)00598-x.

35. Thien, M., Phan, T.G., Gardam, S., Amesbury, M., Basten, A., Mackay, F., and Brink, R. (2004). Excess BAFF Rescues Self-Reactive B Cells from Peripheral Deletion and Allows Them to Enter Forbidden Follicular and Marginal Zone Niches. Immunity *20*, 785–798. 10.1016/j.immuni.2004.05.010.

36. Lesley, R., Xu, Y., Kalled, S.L., Hess, D.M., Schwab, S.R., Shu, H.-B., and Cyster, J.G. (2004). Reduced Competitiveness of Autoantigen-Engaged B Cells due to Increased Dependence on BAFF. Immunity *20*, 441–453. 10.1016/s1074-7613(04)00079-2.

37. Lau, A.W.Y., Turner, V.M., Bourne, K., Hermes, J.R., Chan, T.D., and Brink, R. (2020). BAFFR controls early memory B cell responses but is dispensable for germinal center function. J Exp Med *218*, e20191167. 10.1084/jem.20191167.

38. Müller-Winkler, J., Mitter, R., Rappe, J.C.F., Vanes, L., Schweighoffer, E., Mohammadi, H., Wack, A., and Tybulewicz, V.L.J. (2020). Critical requirement for BCR, BAFF, and BAFFR in memory B cell survival. J Exp Med *218*, e20191393. 10.1084/jem.20191393.

39. Mesin, L., Schiepers, A., Ersching, J., Barbulescu, A., Cavazzoni, C.B., Angelini, A., Okada, T., Kurosaki, T., and Victora, G.D. (2020). Restricted Clonality and Limited Germinal Center Reentry Characterize Memory B Cell Reactivation by Boosting. Cell *180*, 92-106.e11. 10.1016/j.cell.2019.11.032.

40. Ittah, M., Miceli-Richard, C., Lebon, P., Pallier, C., Lepajolec, C., and Mariette, X. (2011). Induction of B Cell-Activating Factor by Viral Infection Is a General Phenomenon, but the Types of Viruses and Mechanisms Depend on Cell Type. J Innate Immun *3*, 200–207. 10.1159/000321194.

Fig 1

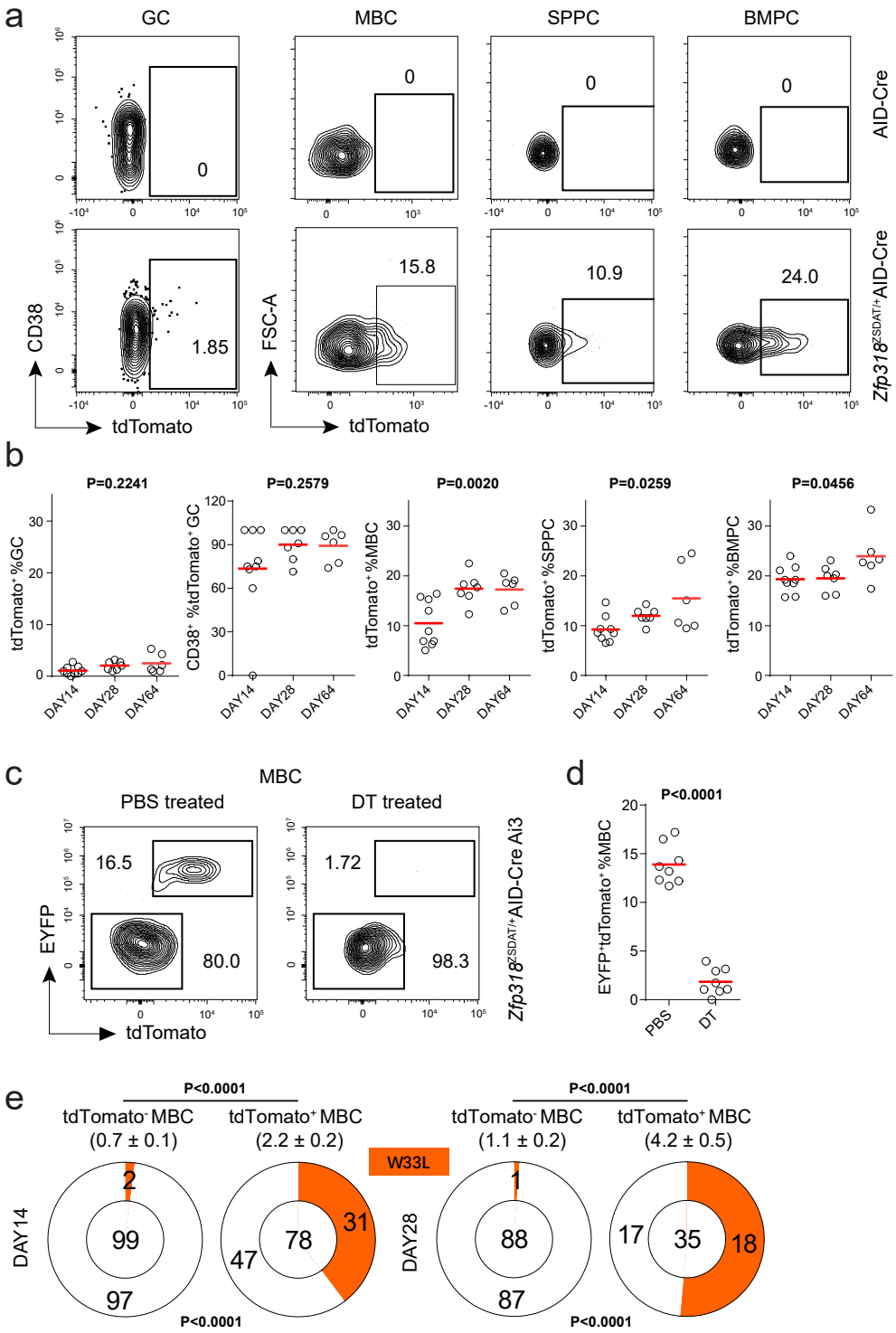
a
GC
MBC
SPPC
BMPC
AID-Cre
Zfp318ZSDAT/+AID-Cre
CD38
FSC-A
tdTomato
0
1.85
15.8
10.9
24.0
b
P=0.2241
P=0.2579
P=0.0020
P=0.0259
P=0.0456
tdTomato+%GC
CD38+ %tdTomato+ GC
tdTomato+%MBC
tdTomato+%SPPC
tdTomato+%BMPC
DAY14
DAY28
DAY64
c
MBC
PBS treated
DT treated
EYFP
16.5
80.0
1.72
98.3
Zfp318ZSDAT/+AID-Cre Ai3
d
P<0.0001
EYFP+tdTomato+%MBC
PBS
DT
e
P<0.0001
tdTomato- MBC
(0.7 ± 0.1)
tdTomato+ MBC
(2.2 ± 0.2)
tdTomato- MBC
(1.1 ± 0.2)
tdTomato+ MBC
(4.2 ± 0.5)
W33L
DAY14
DAY28
2
99
97
31
78
47
1
88
87
17
35
18

Fig 2

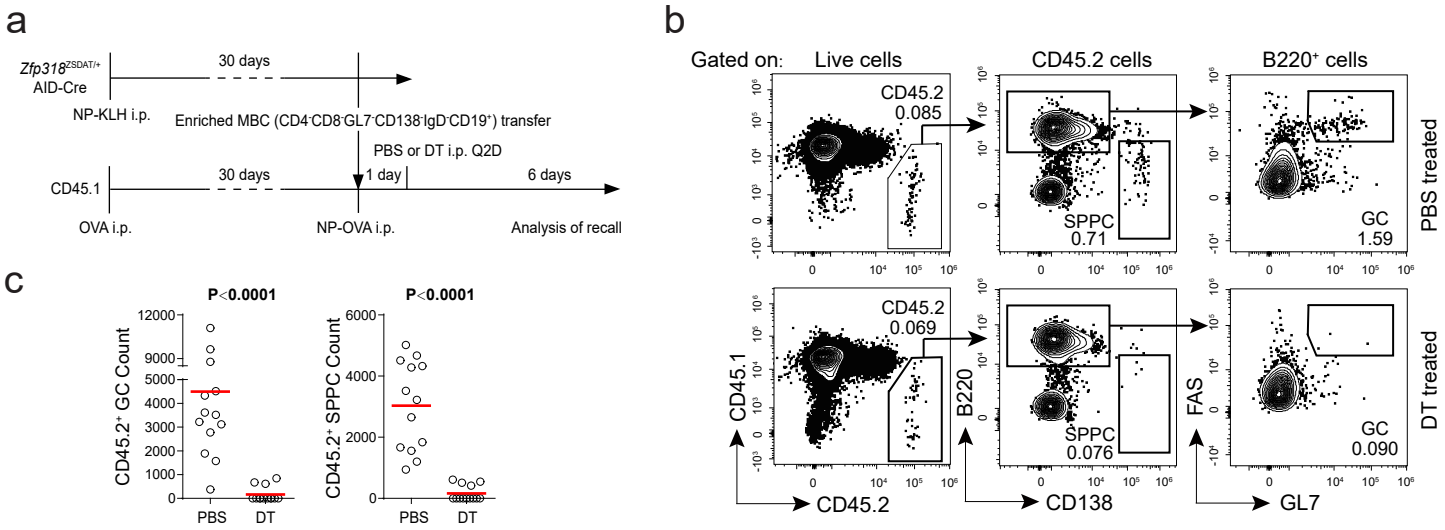
a
Zfp318ZSDAT/+
AID-Cre
30 days
NP-KLH i.p.
Enriched MBC (CD4-CD8-GL7-CD138-IgD-CD19+) transfer
PBS or DT i.p. Q2D
CD45.1
30 days
1 day
6 days
OVA i.p.
NP-OVA i.p.
Analysis of recall
b
Gated on:
Live cells
CD45.2 cells
B220+ cells
CD45.2
0.085
SPPC
0.71
GC
1.59
PBS treated
CD45.2
0.069
SPPC
0.076
GC
0.090
DT treated
CD45.1
CD45.2
B220
CD138
FAS
GL7
c
P<0.0001
CD45.2+ GC Count
PBS
DT
P<0.0001
CD45.2+ SPPC Count
PBS
DT

Fig 3

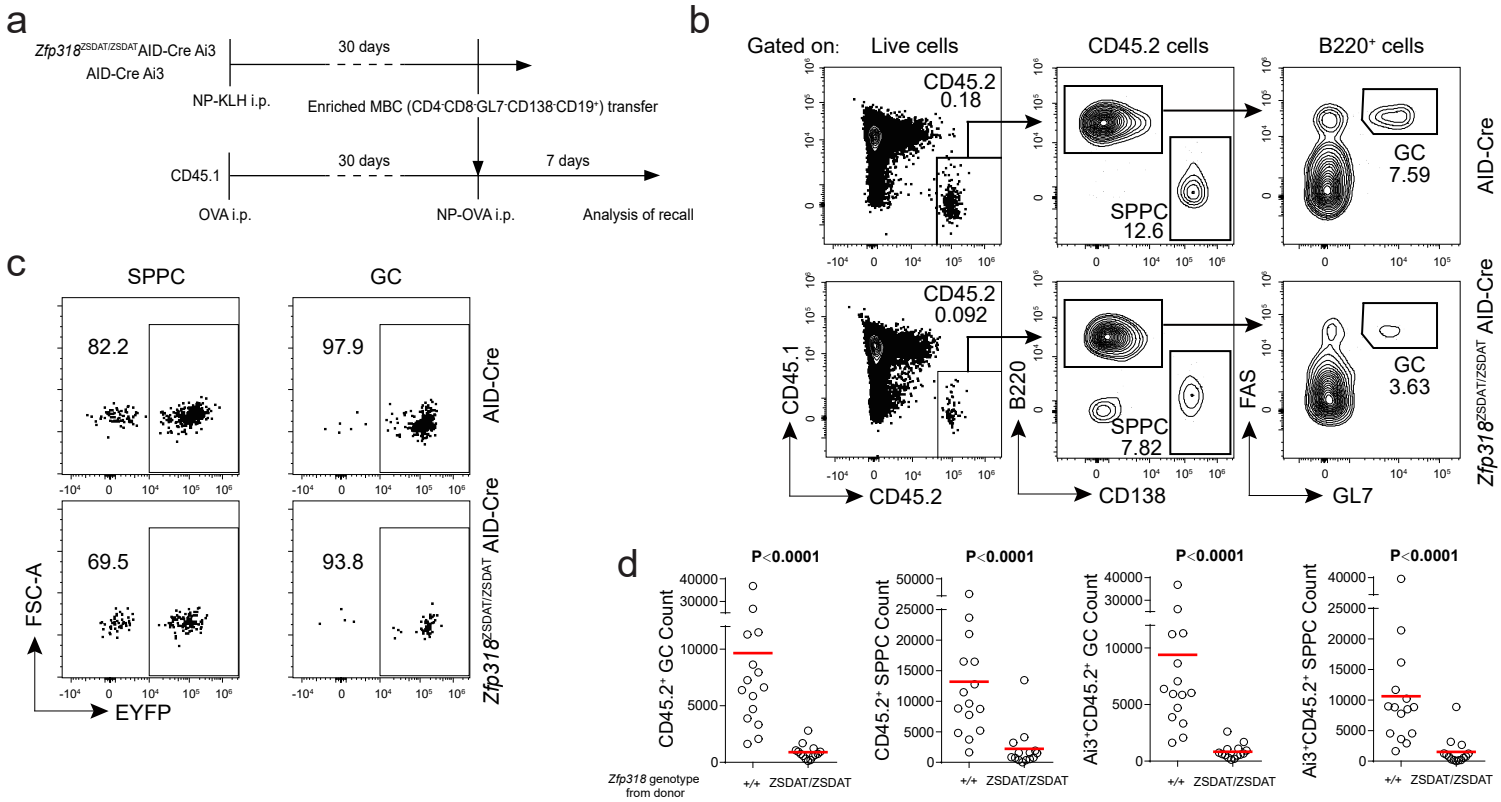
a
Zfp318ZSDAT/ZSDAT AID-Cre Ai3
AID-Cre Ai3
30 days
NP-KLH i.p.
Enriched MBC (CD4-CD8-GL7-CD138-CD19+) transfer
CD45.1
30 days
7 days
OVA i.p.
NP-OVA i.p.
Analysis of recall
b
Gated on:
Live cells
CD45.2 cells
B220+ cells
CD45.2
0.18
SPPC
12.6
GC
7.59
AID-Cre
CD45.2
0.092
SPPC
7.82
GC
3.63
Zfp318ZSDAT/ZSDAT AID-Cre
CD45.1
CD45.2
B220
CD138
FAS
GL7
c
SPPC
GC
82.2
97.9
AID-Cre
69.5
93.8
Zfp318ZSDAT/ZSDAT AID-Cre
FSC-A
EYFP
d
P<0.0001
CD45.2+ GC Count
CD45.2+ SPPC Count
Ai3+CD45.2+ GC Count
Ai3+CD45.2+ SPPC Count
Zfp318 genotype from donor
+/+
ZSDAT/ZSDAT

Fig 4

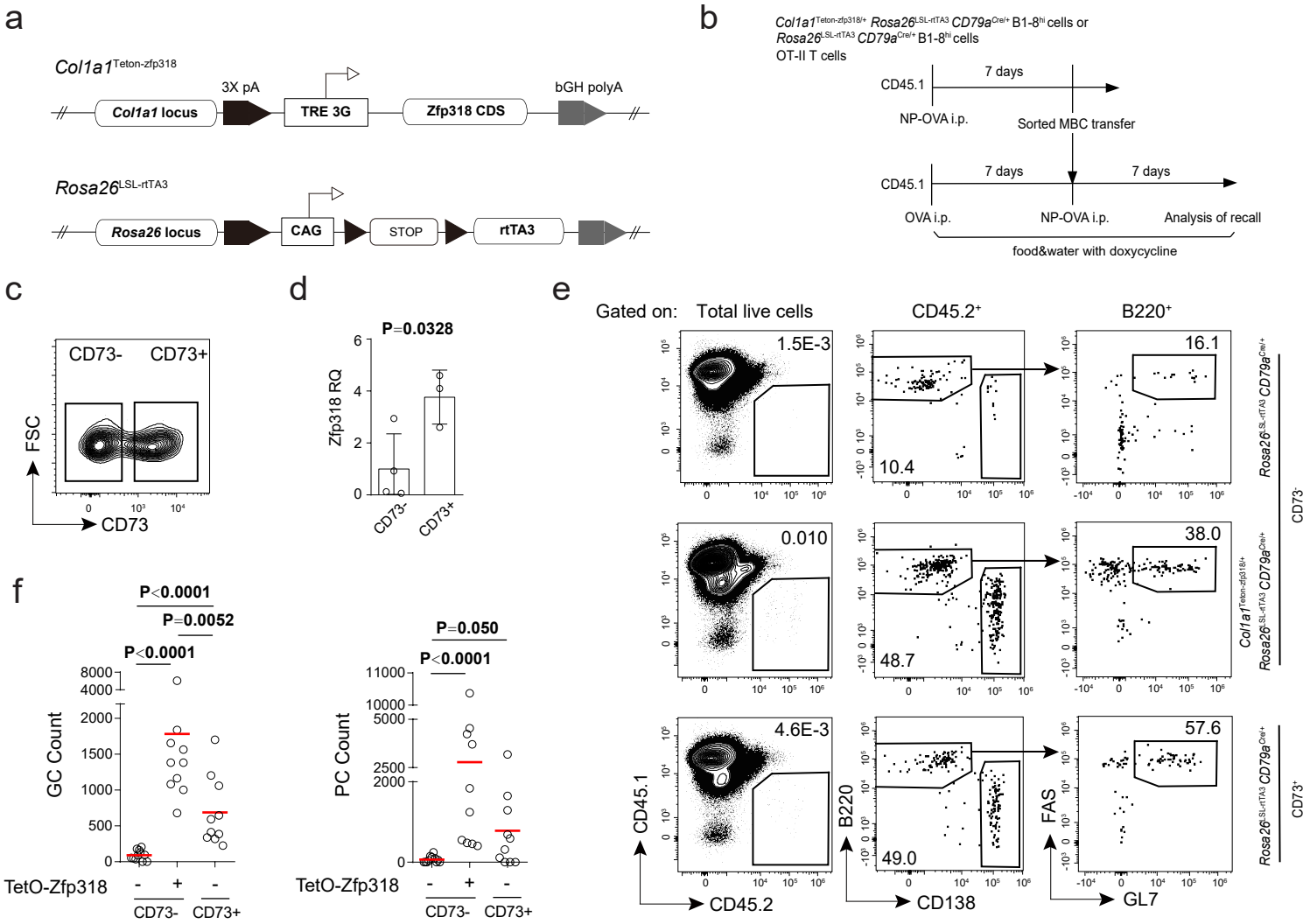
a
Col1a1Teton-zfp318
3X pA
TRE 3G
Zfp318 CDS
bGH polyA
Col1a1 locus
Rosa26LSL-rtTA3
CAG
STOP
rtTA3
Rosa26 locus
b
Col1a1Teton-zfp318/+ Rosa26LSL-rtTA3 CD79aCre/+ B1-8hi cells or
Rosa26LSL-rtTA3 CD79aCre/+ B1-8hi cells
OT-II T cells
CD45.1
7 days
NP-OVA i.p.
Sorted MBC transfer
CD45.1
7 days
7 days
OVA i.p.
NP-OVA i.p.
Analysis of recall
food&water with doxycycline
c
CD73-
CD73+
FSC
CD73
d
P=0.0328
Zfp318 RQ
CD73-
CD73+
e
Gated on:
Total live cells
CD45.2+
B220+
1.5E-3
10.4
16.1
0.010
48.7
38.0
4.6E-3
49.0
57.6
CD45.1
CD45.2
B220
CD138
FAS
GL7
Rosa26LSL-rtTA3 CD79aCre/+
Col1a1Teton-zfp318/+
Rosa26LSL-rtTA3 CD79aCre/+
Rosa26LSL-rtTA3 CD79aCre/+
CD73-
CD73+
f
P<0.0001
P=0.0052
P<0.0001
GC Count
TetO-Zfp318
CD73-
CD73+
P=0.050
P<0.0001
PC Count
TetO-Zfp318
CD73-
CD73+

Fig 5

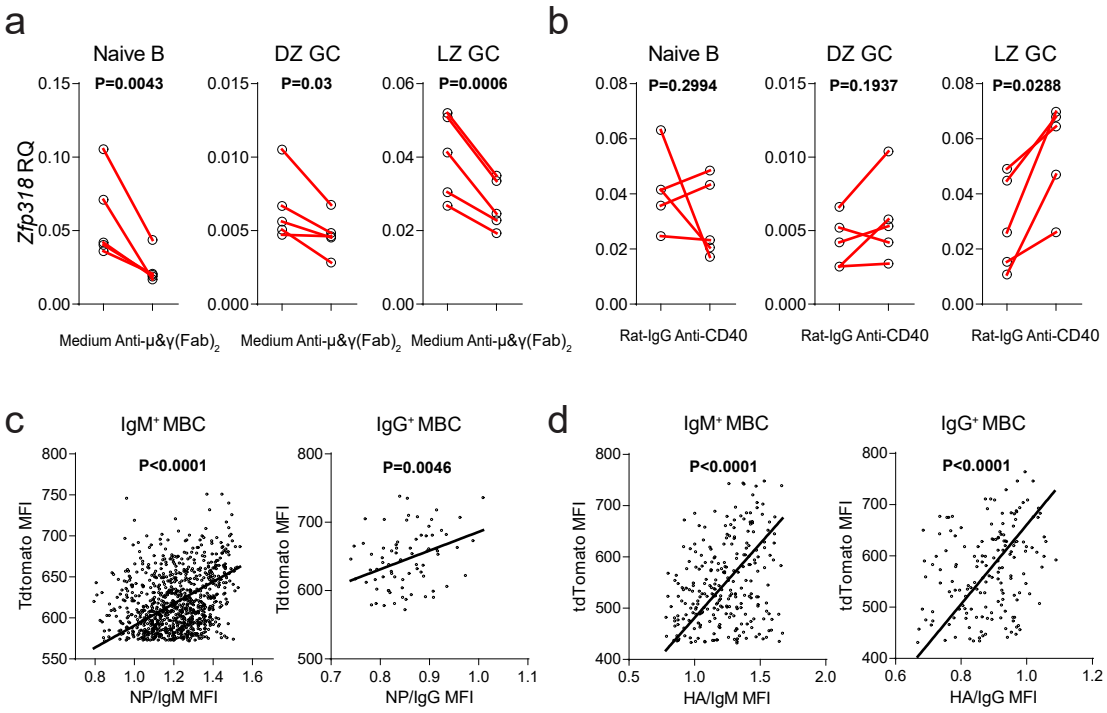
a
Naive B
DZ GC
LZ GC
P=0.0043
P=0.03
P=0.0006
Zfp318 RQ
Medium Anti-μ&γ(Fab)2
b
P=0.2994
P=0.1937
P=0.0288
Rat-IgG Anti-CD40
c
IgM+ MBC
IgG+ MBC
P<0.0001
P=0.0046
Tdtomato MFI
NP/IgM MFI
NP/IgG MFI
d
tdTomato MFI
HA/IgM MFI
HA/IgG MFI

Fig 6

a

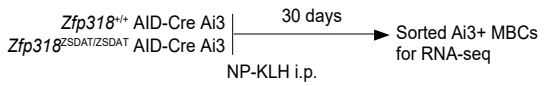

b

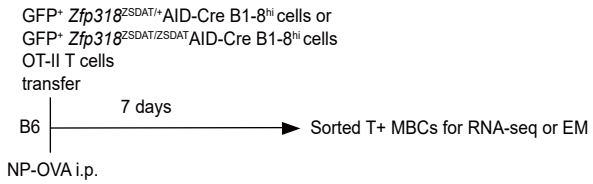

c

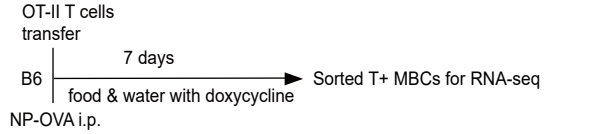

d

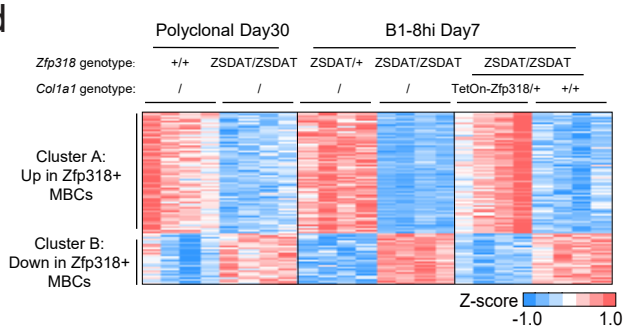

e

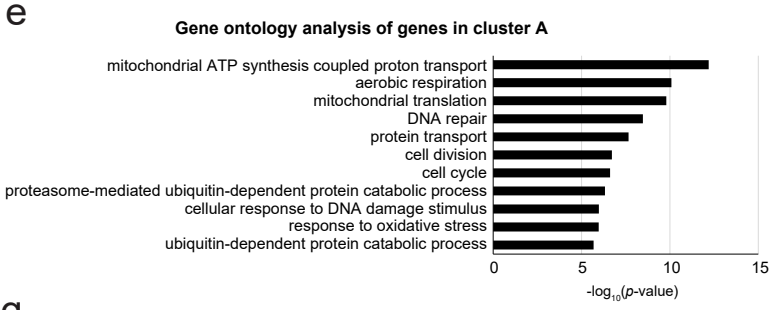

f

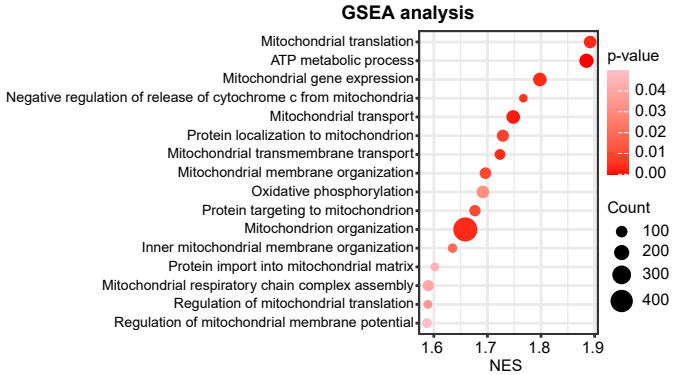

g

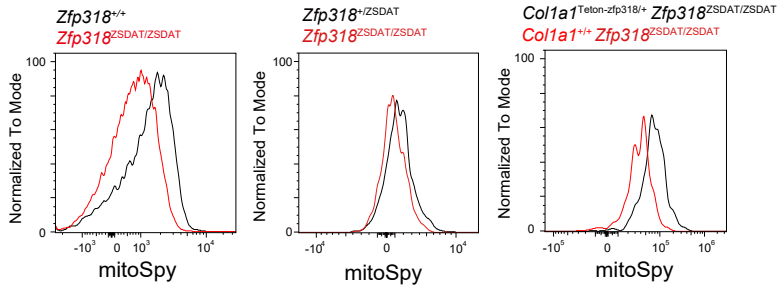

h

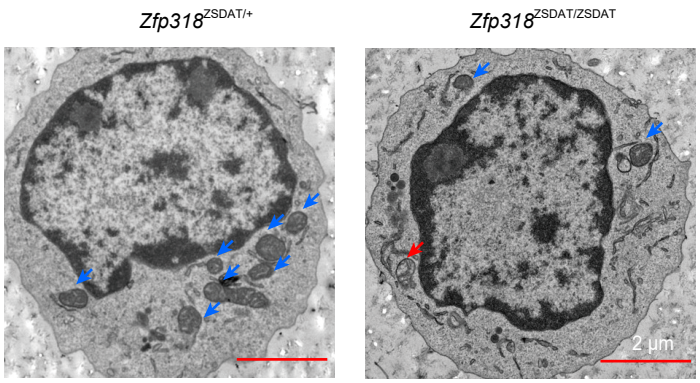

i

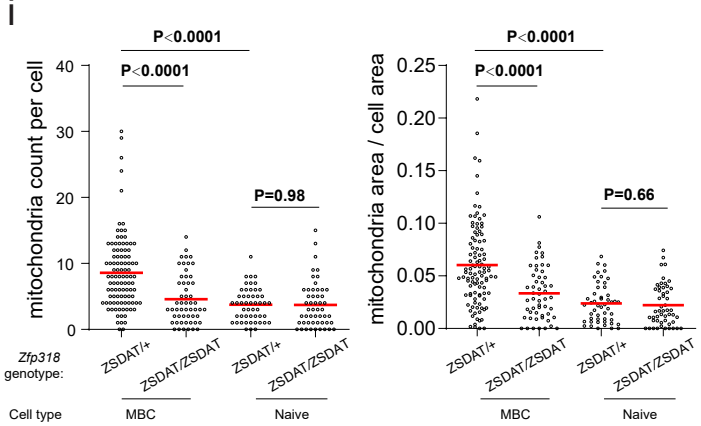

j

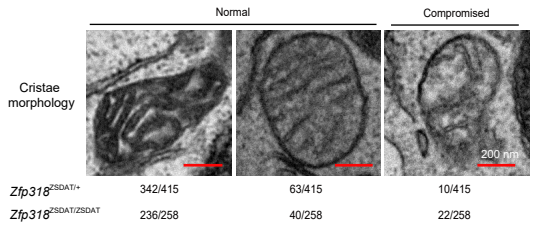

k

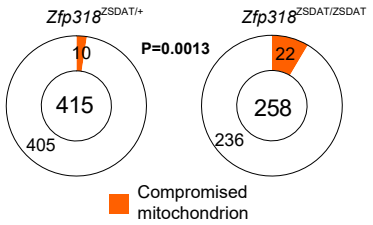

l

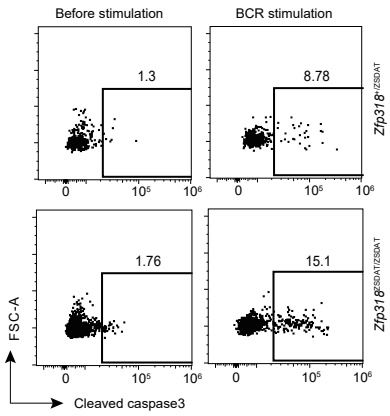

m

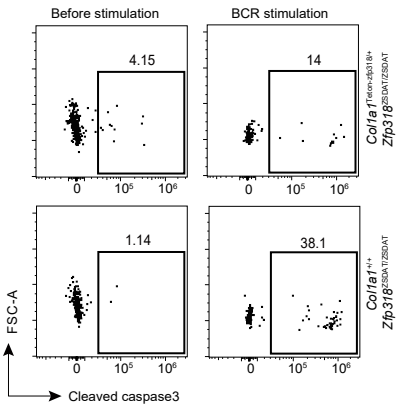

Fig.7

a

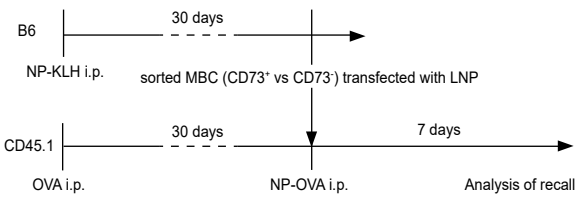
B6
30 days
NP-KLH i.p.
sorted MBC (CD73+ vs CD73-) transfected with LNP
CD45.1
30 days
7 days
OVA i.p.
NP-OVA i.p.
Analysis of recall

c

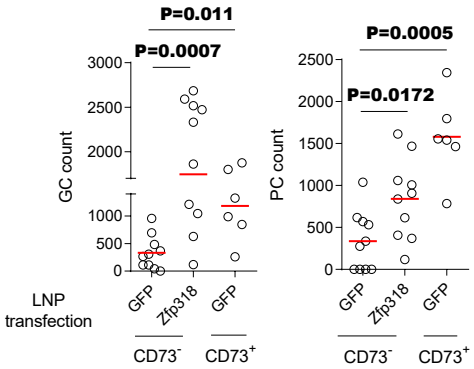
P=0.011
P=0.0007
GC count
LNP transfection
GFP
Zfp318
GFP
CD73-
CD73+
P=0.0005
P=0.0172
PC count
GFP
Zfp318
GFP
CD73-
CD73+

b

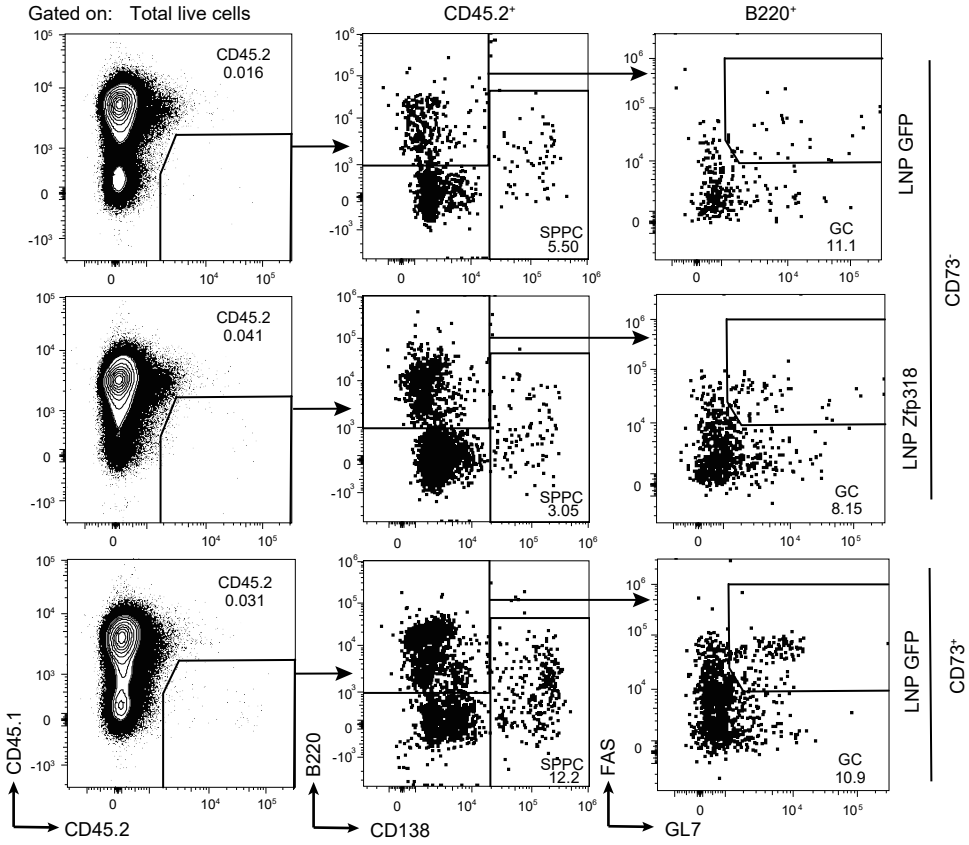
Gated on: Total live cells
CD45.2+
B220+
CD45.2
0.016
SPPC
5.50
GC
11.1
LNP GFP
CD73-
CD45.2
0.041
SPPC
3.05
GC
8.15
LNP Zfp318
CD45.2
0.031
SPPC
12.2
GC
10.9
LNP GFP
CD73+
CD45.1
CD45.2
B220
CD138
FAS
GL7

Fig.S1

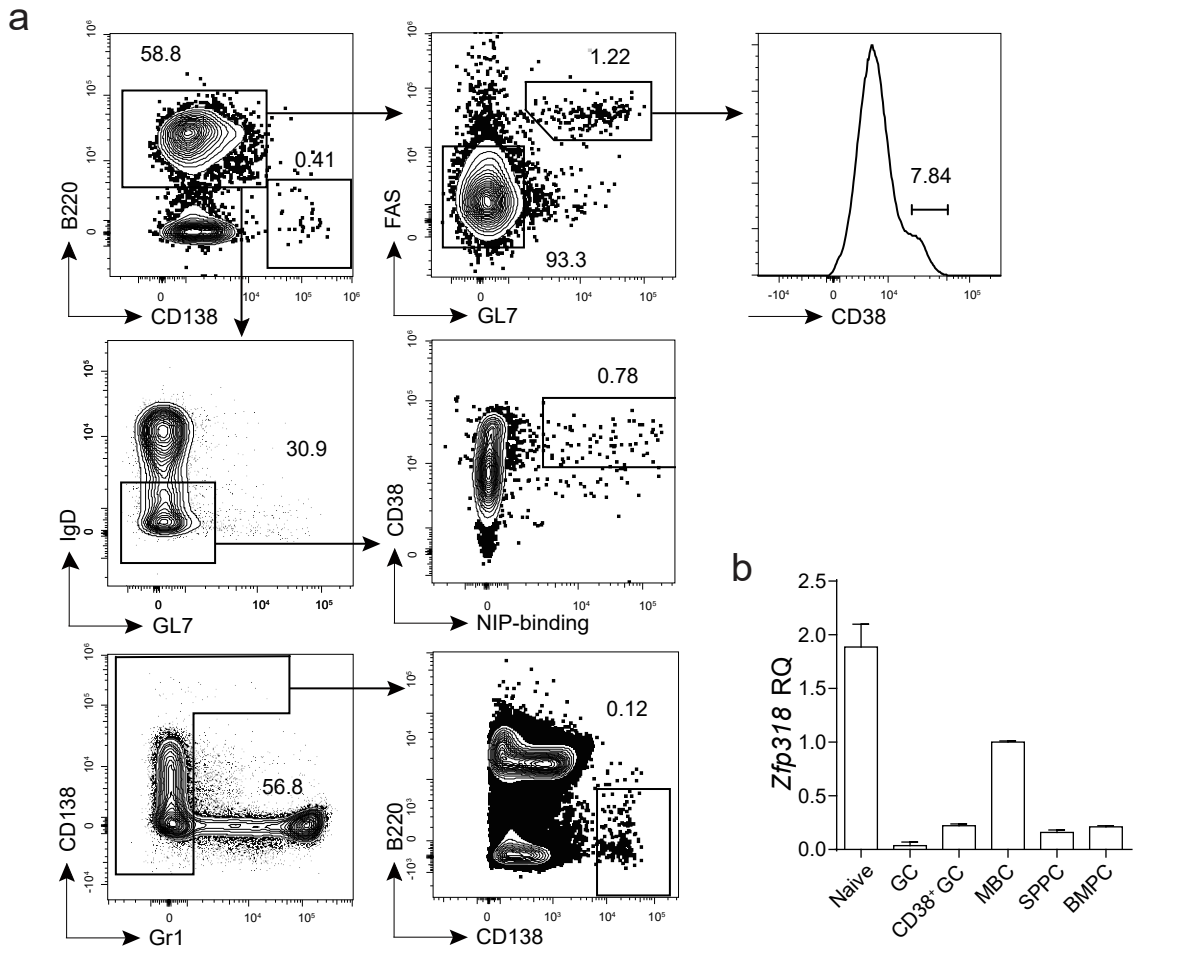
a
58.8
0.41
B220
CD138
1.22
93.3
FAS
GL7
7.84
CD38
30.9
IgD
GL7
0.78
CD38
NIP-binding
56.8
CD138
Gr1
0.12
B220
CD138
b
Zfp318 RQ
2.5
2.0
1.5
1.0
0.5
0.0
Naive
GC
CD38+ GC
MBC
SPPC
BMPC

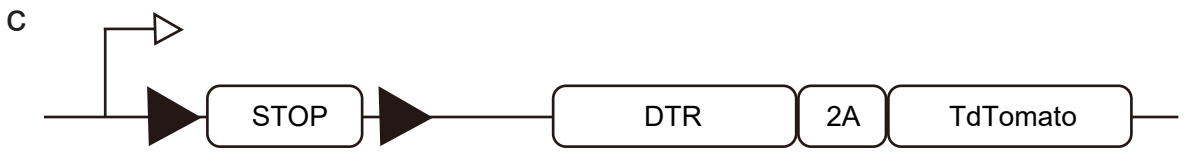
c
STOP
DTR
2A
TdTomato

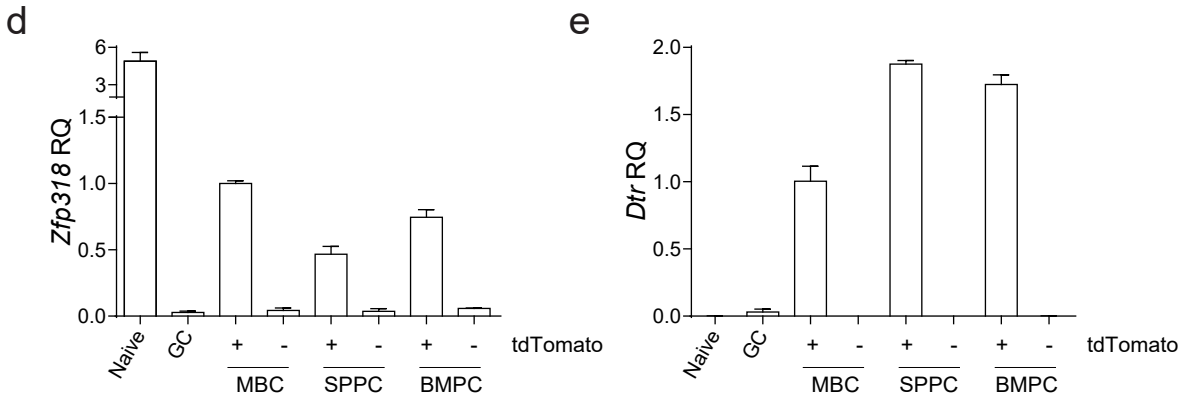
d
Zfp318 RQ
6
3
1.5
1.0
0.5
0.0
Naive
GC
+
-
+
-
+
-
tdTomato
MBC
SPPC
BMPC
e
Dtr RQ
2.0
1.5
1.0
0.5
0.0
Naive
GC
+
-
+
-
+
-
tdTomato
MBC
SPPC
BMPC

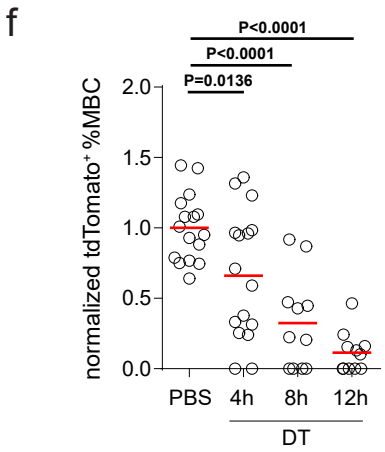
f
P<0.0001
P<0.0001
P=0.0136
normalized tdTomato+ %MBC
2.0
1.5
1.0
0.5
0.0
PBS
4h
8h
12h
DT

Fig.S2

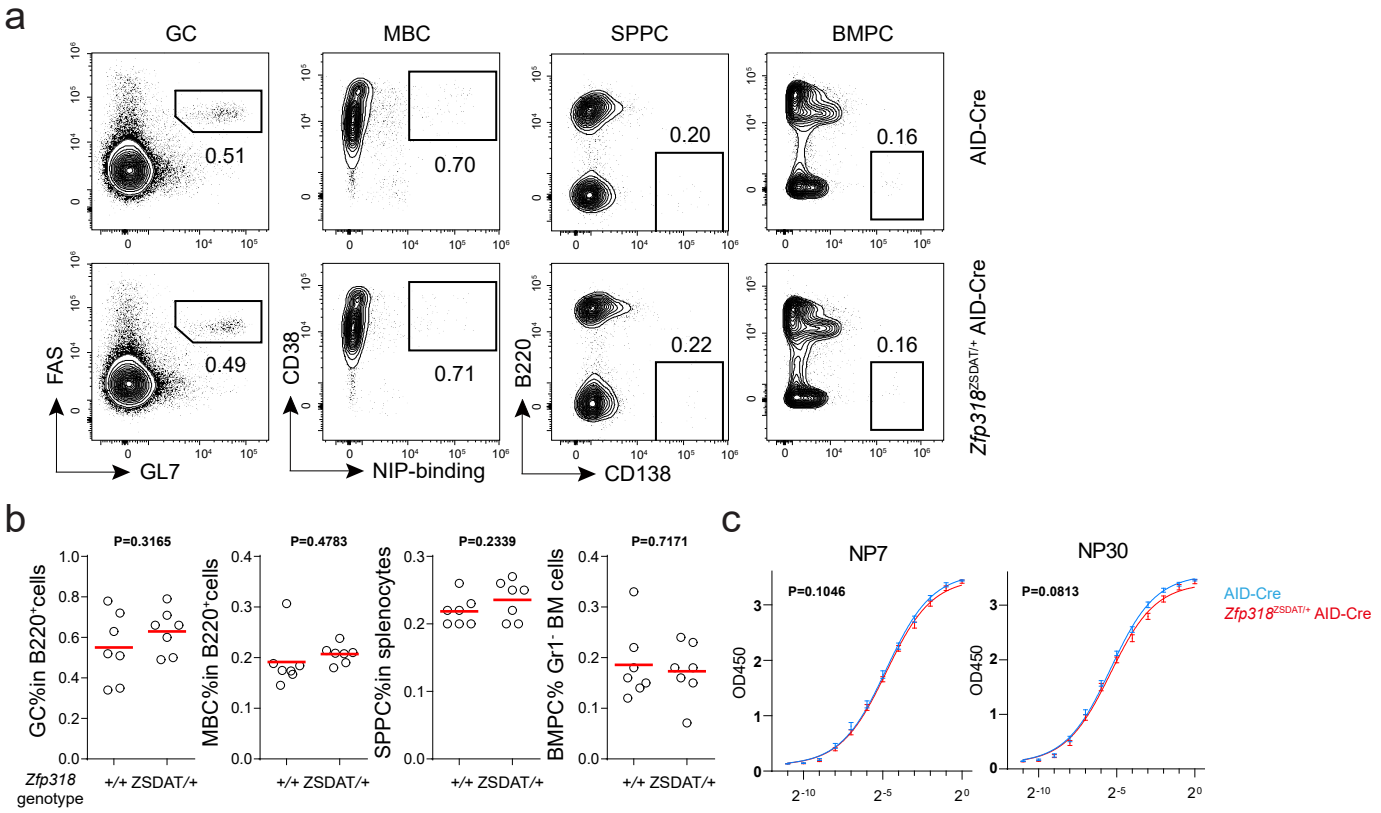
a
GC
MBC
SPPC
BMPC
0.51
0.70
0.20
0.16
AID-Cre
0.49
0.71
0.22
0.16
Zfp318ZSDAT/+ AID-Cre
FAS
GL7
CD38
NIP-binding
B220
CD138
b
P=0.3165
P=0.4783
P=0.2339
P=0.7171
GC%in B220+cells
MBC%in B220+cells
SPPC%in splenocytes
BMPC% Gr1- BM cells
Zfp318 genotype
+/+ ZSDAT/+
c
NP7
NP30
P=0.1046
P=0.0813
OD450
AID-Cre
Zfp318ZSDAT/+ AID-Cre

Fig.S3

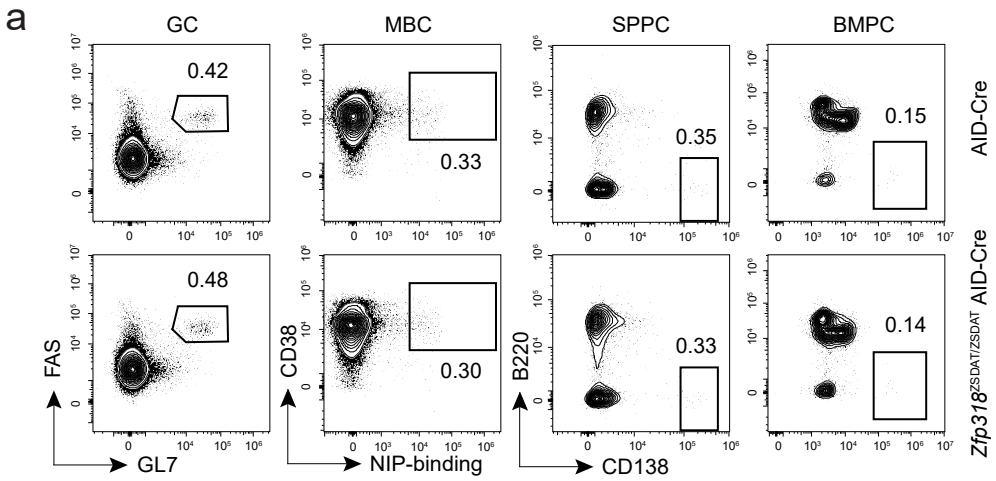
a
GC
MBC
SPPC
BMPC
0.42
0.33
0.35
0.15
AID-Cre
0.48
0.30
0.33
0.14
Zfp318ZSDAT/ZSDAT AID-Cre
FAS
GL7
CD38
NIP-binding
B220
CD138

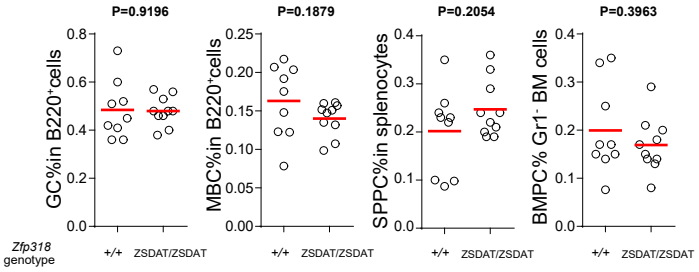
b
P=0.9196
P=0.1879
P=0.2054
P=0.3963
GC%in B220+cells
MBC%in B220+cells
SPPC%in splenocytes
BMPC% Gr1- BM cells
Zfp318 genotype
+/+
ZSDAT/ZSDAT

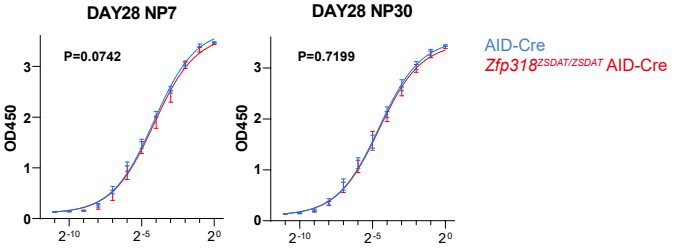
c
DAY28 NP7
DAY28 NP30
P=0.0742
P=0.7199
OD450
AID-Cre
Zfp318ZSDAT/ZSDAT AID-Cre

Fig.S4

a

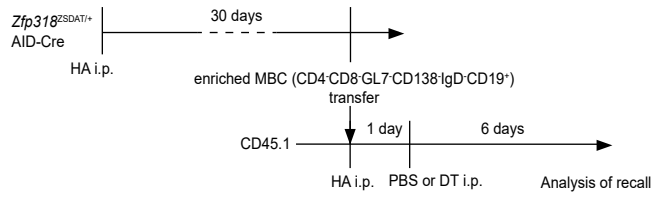
Zfp318ZSDAT/+
AID-Cre
HA i.p.
30 days
enriched MBC (CD4-CD8-GL7-CD138-IgD-CD19+)
transfer
CD45.1
1 day
6 days
HA i.p.
PBS or DT i.p.
Analysis of recall

c

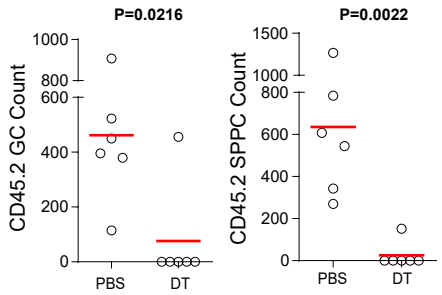
P=0.0216
P=0.0022
CD45.2 GC Count
CD45.2 SPPC Count
PBS
DT

b

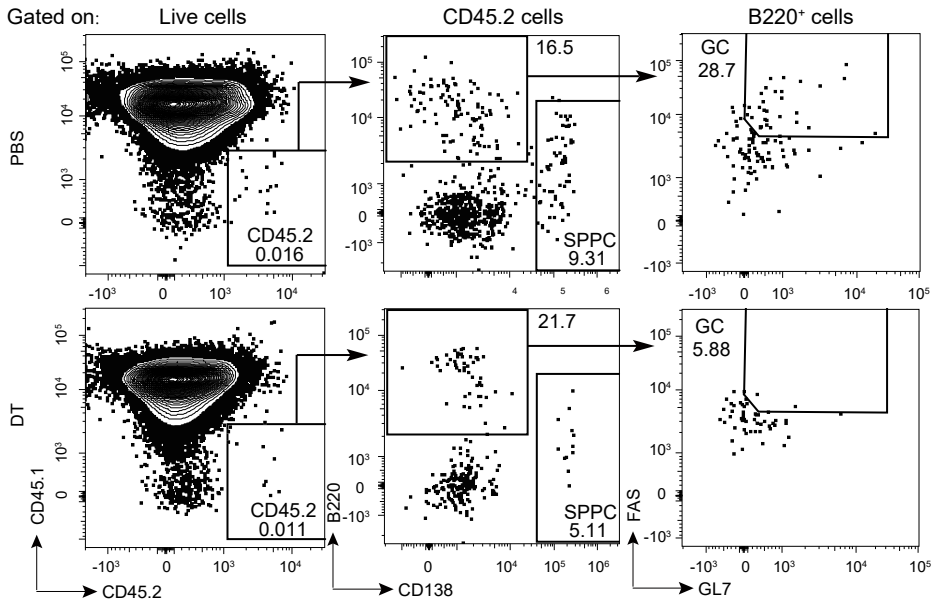
Gated on:
Live cells
CD45.2 cells
B220+ cells
PBS
DT
CD45.2
0.016
16.5
SPPC
9.31
GC
28.7
CD45.2
0.011
21.7
SPPC
5.11
GC
5.88
CD45.1
CD45.2
B220
CD138
FAS
GL7

Fig.S5

a

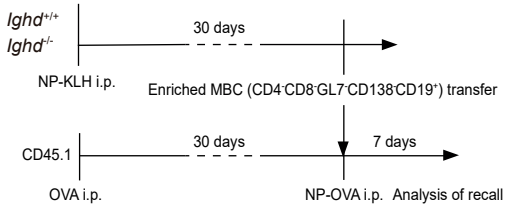
Ighd+/+
Ighd-/-
30 days
NP-KLH i.p.
Enriched MBC (CD4-CD8-GL7-CD138-CD19+) transfer
CD45.1
30 days
7 days
OVA i.p.
NP-OVA i.p. Analysis of recall

b

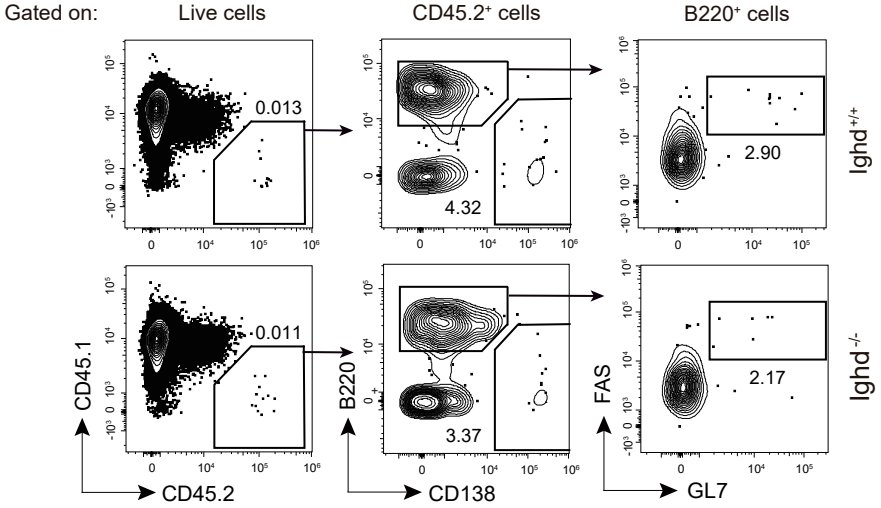
Gated on:
Live cells
CD45.2+ cells
B220+ cells
0.013
4.32
2.90
Ighd+/+
0.011
3.37
2.17
Ighd-/-
CD45.1
CD45.2
B220
CD138
FAS
GL7

c

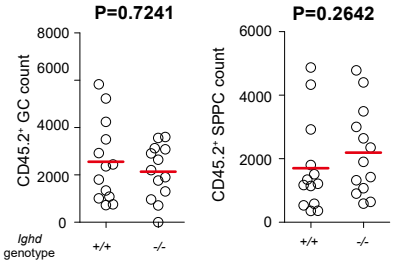
P=0.7241
P=0.2642
CD45.2+ GC count
CD45.2+ SPPC count
8000
6000
4000
2000
0
Ighd genotype
+/+
-/-

Fig.S6

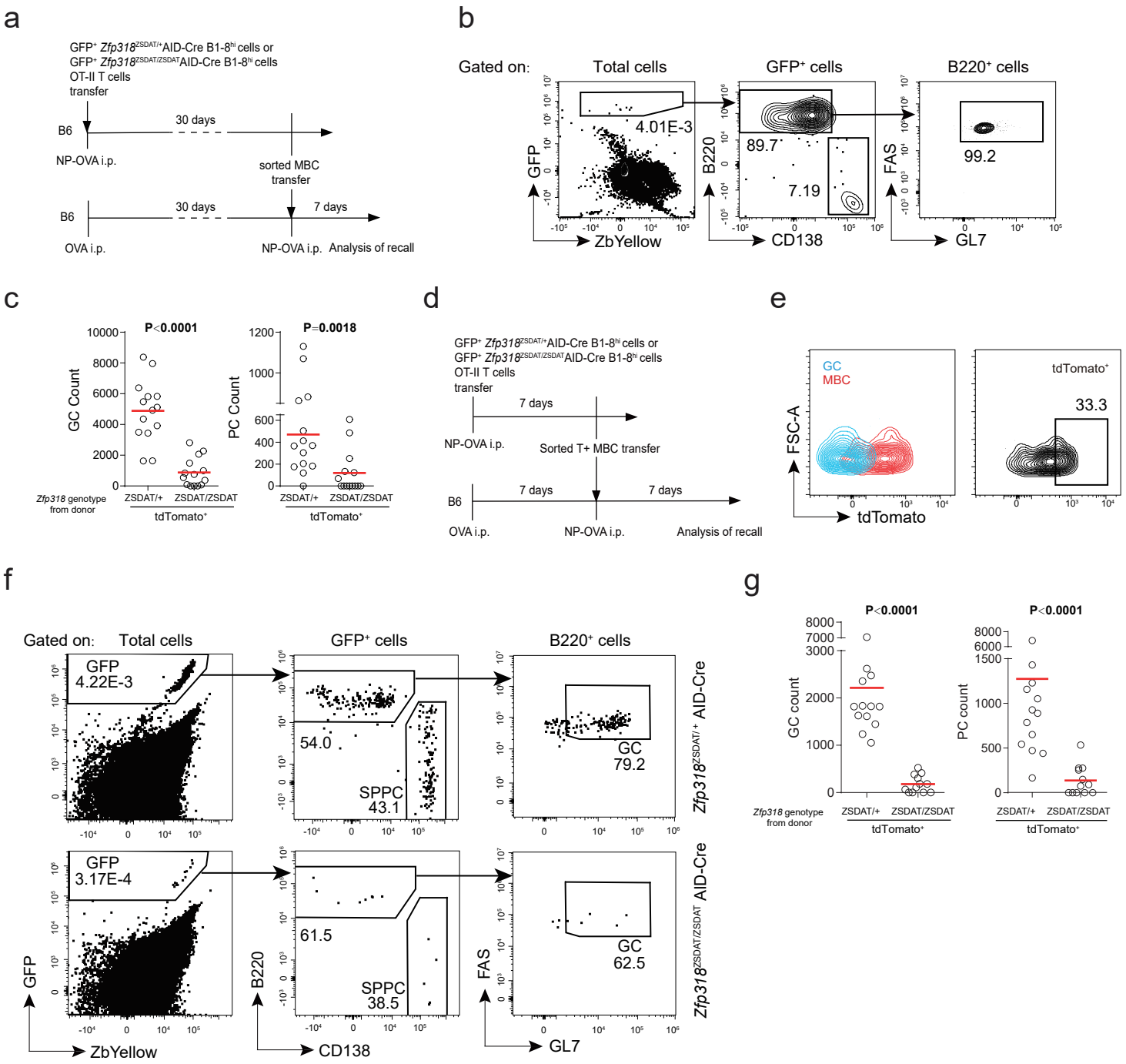
a
GFP+ Zfp318ZSDAT/+AID-Cre B1-8hi cells or
GFP+ Zfp318ZSDAT/ZSDATAID-Cre B1-8hi cells
OT-II T cells
transfer
B6
30 days
NP-OVA i.p.
sorted MBC
transfer
B6
30 days
7 days
OVA i.p.
NP-OVA i.p.
Analysis of recall
b
Gated on:
Total cells
GFP+ cells
B220+ cells
4.01E-3
89.7
7.19
99.2
GFP
ZbYellow
B220
CD138
FAS
GL7
c
P<0.0001
P=0.0018
GC Count
PC Count
Zfp318 genotype
from donor
ZSDAT/+
ZSDAT/ZSDAT
tdTomato+
d
GFP+ Zfp318ZSDAT/+AID-Cre B1-8hi cells or
GFP+ Zfp318ZSDAT/ZSDATAID-Cre B1-8hi cells
OT-II T cells
transfer
7 days
NP-OVA i.p.
Sorted T+ MBC transfer
B6
7 days
7 days
OVA i.p.
NP-OVA i.p.
Analysis of recall
e
GC
MBC
FSC-A
tdTomato
tdTomato+
33.3
f
Gated on:
Total cells
GFP+ cells
B220+ cells
GFP
4.22E-3
54.0
SPPC
43.1
GC
79.2
Zfp318ZSDAT/+ AID-Cre
GFP
3.17E-4
61.5
SPPC
38.5
GC
62.5
Zfp318ZSDAT/ZSDAT AID-Cre
GFP
ZbYellow
B220
CD138
FAS
GL7
g
P<0.0001
P<0.0001
GC count
PC count
Zfp318 genotype
from donor
ZSDAT/+
ZSDAT/ZSDAT
tdTomato+

Fig.S7

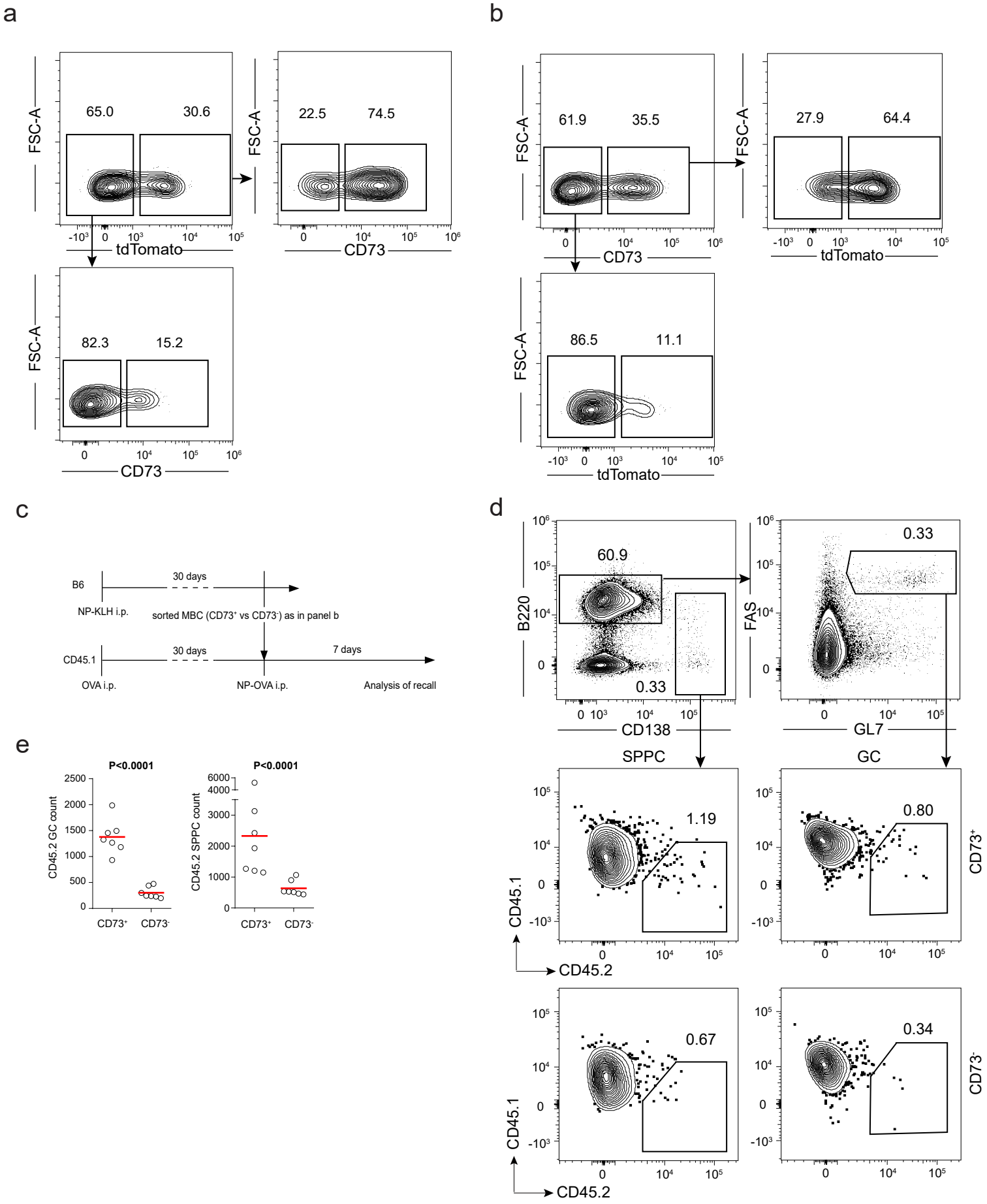
a
FSC-A
65.0
30.6
tdTomato
22.5
74.5
CD73
82.3
15.2
b
61.9
35.5
27.9
64.4
86.5
11.1
c
B6
30 days
NP-KLH i.p.
sorted MBC (CD73+ vs CD73-) as in panel b
CD45.1
7 days
OVA i.p.
NP-OVA i.p.
Analysis of recall
d
B220
CD138
FAS
GL7
60.9
0.33
SPPC
GC
1.19
0.80
0.67
0.34
CD45.1
CD45.2
CD73+
CD73-
e
P<0.0001
CD45.2 GC count
CD45.2 SPPC count

Fig S8

a

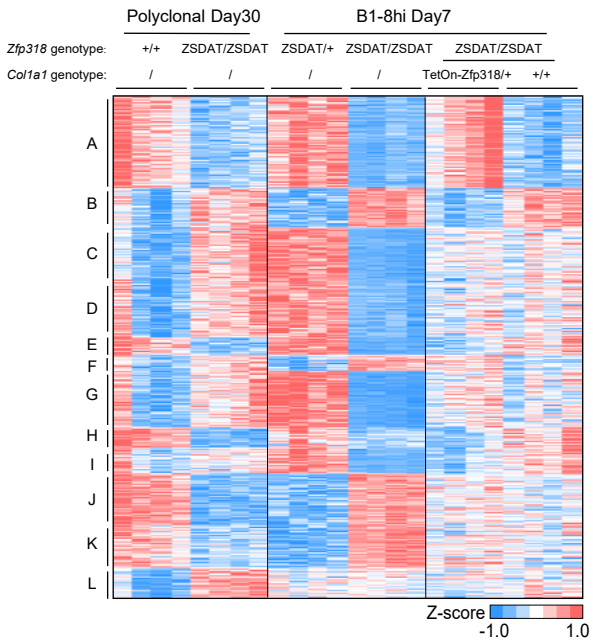

b

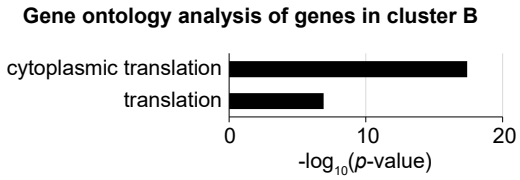

c

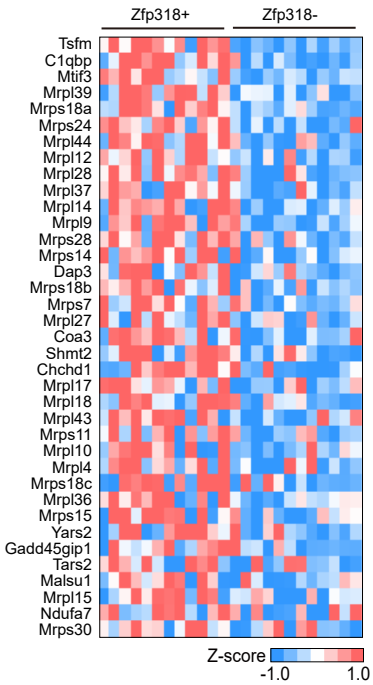

d

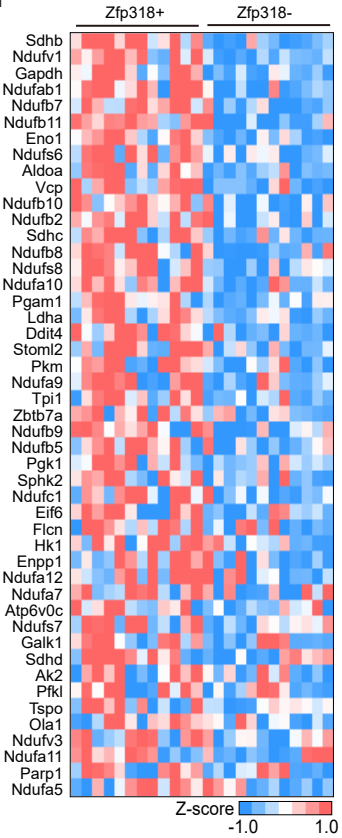

e

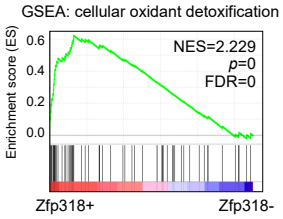

f

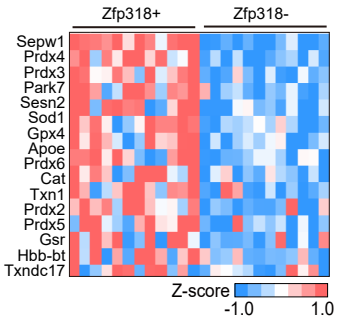

g

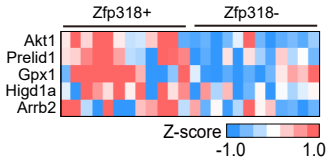

h

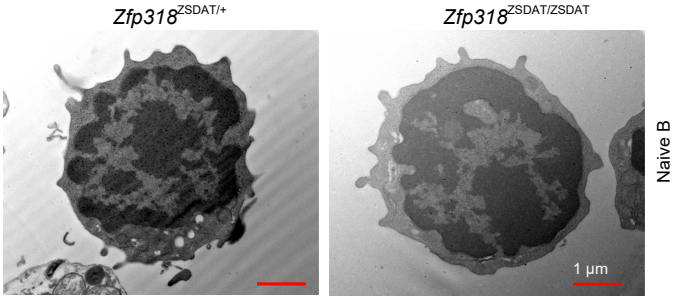

Fig.S9

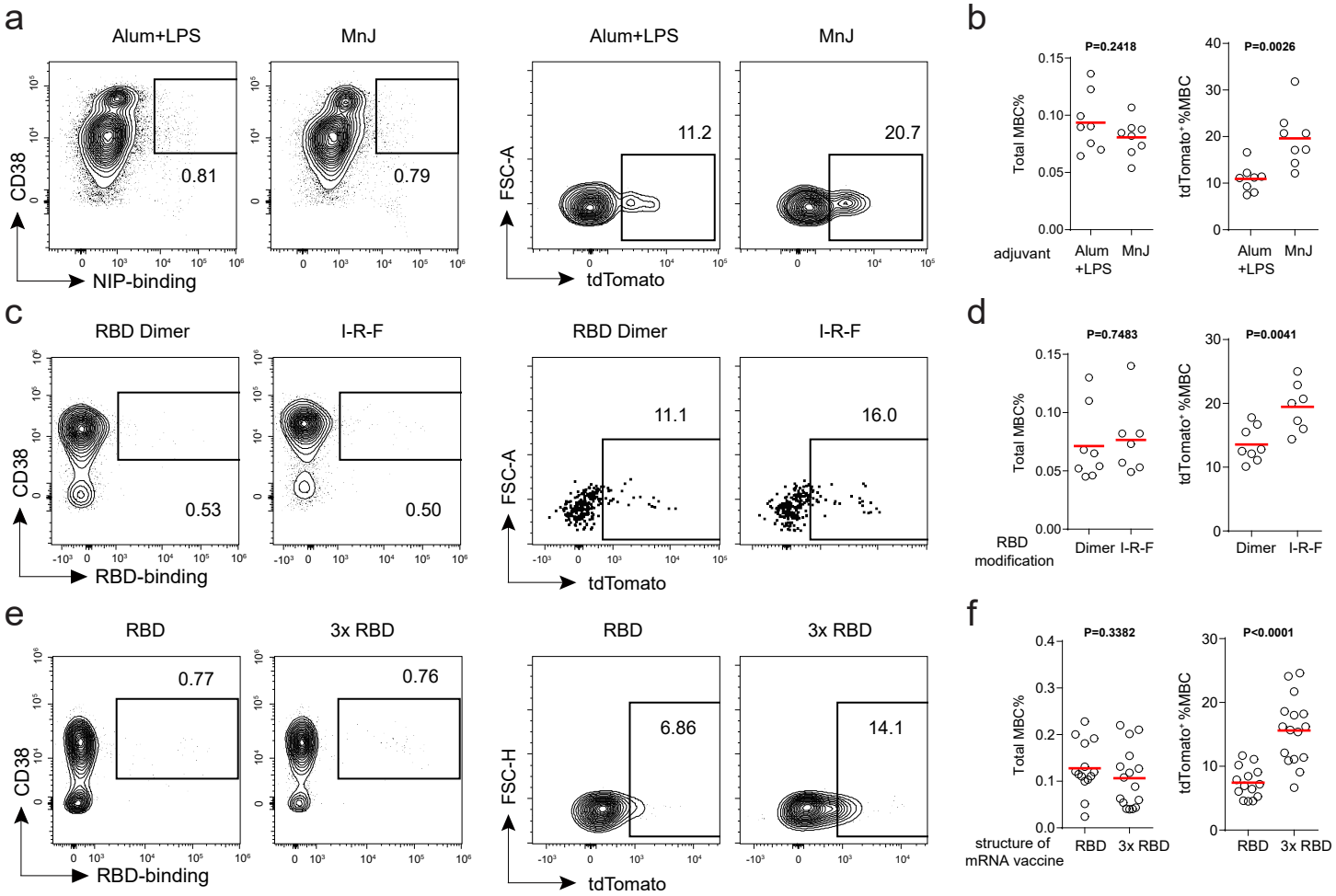
a
Alum+LPS
MnJ
Alum+LPS
MnJ
CD38
NIP-binding
0.81
0.79
FSC-A
tdTomato
11.2
20.7
b
P=0.2418
P=0.0026
Total MBC%
tdTomato+%MBC
adjuvant
Alum +LPS
MnJ
c
RBD Dimer
I-R-F
RBD Dimer
I-R-F
CD38
RBD-binding
0.53
0.50
FSC-A
tdTomato
11.1
16.0
d
P=0.7483
P=0.0041
Total MBC%
tdTomato+%MBC
RBD modification
Dimer
I-R-F
e
RBD
3x RBD
RBD
3x RBD
CD38
RBD-binding
0.77
0.76
FSC-H
tdTomato
6.86
14.1
f
P=0.3382
P<0.0001
Total MBC%
tdTomato+%MBC
structure of mRNA vaccine
RBD
3x RBD